Preliminary Copy
WADC TR 54-175
Part 2

NOTCH SENSITIVITY OF HEAT-RESISTANT ALLOYS AT ELEVATED TEMPERATURES

Part 2 Analysis of Notched-Bar Rupture Life in Terms of Smooth-Bar Properties

Howard R. Voorhees
James W. Freeman

University of Michigan

December 1954

Materials Laboratory
Contract No. AF 18(600)-62
RDO No. 614-13 MC
Subtask 73605 (J)

Wright Air Development Center
Air Research and Development Command
United States Air Force
Wright-Patterson Air Force Base, Ohio

FOREWORD

This report was prepared by the University of Michigan, under USAF Contract No. AF 18(600)-62. The contract was initiated under Research and Development Order No. 614-13 MC, "Design and Evaluation Data for Structural Metals", and has been continued under Subtask 73605 (J), "Notched Creep Rupture". The research was administered under the direction of the Materials Laboratory, Directorate of Research, Wright Air Development Center, with Dr. A. Herzog acting as project engineer. This report covers work performed during calendar year 1954.

ABSTRACT

Rupture lives of smooth and notched bars have been compared in tests on three heat-resistant alloys with conventional heat treatments. Additional rupture tests were run for two of the alloys using notched and smooth specimens from material cold rolled between solution and aging treatments. The method of notch preparation was demonstrated to have a large effect on notched-bar life for some conditions. Variable results were attributed to residual stresses remaining from the machining operation.

Other experimental data obtained on smooth bars for the same alloys and conditions included short-time tensile properties, creep curves, relaxation characteristics, and rupture life when the stress was changed from one level to another during the test.

A definite qualitative agreement was noted between notch strengthening or weakening and the rate of experimental stress relaxation under creep conditions. A quantitative stepwise analysis was developed to compare notch rupture behavior with properties of smooth bars. This analysis was based on the postulate that for a material to be notch strengthened it must be able to relax high initial stress concentrations quickly before a major portion of the total life has been expended in fibers initially at stresses above the nominal stress applied to the specimen. Further, the effective stress in such fibers must eventually drop below the nominal stress for notch strengthening to occur.

Calculation steps in the proposed analysis are summarized on the following page.

Completed calculations for one condition of notch strengthening and one of notch weakening showed satisfactory agreement with experimental findings and indicates that stress redistribution by creep-relaxation could by itself explain the wide differences in notch behavior observed for different materials and test conditions.

Further work is indicated to ascertain influence of other factors and to establish the range of validity of the proposed analytical method. Suggested extensions include tests on flat notched bars and use of other types of alloys.

PUBLICATION REVIEW

This report has been reviewed and is approved

FOR THE COMMANDER:

M. R. WHITMORE
Technical Director
Materials Laboratory
Directorate of Research

SUMMARY OF PROPOSED CALCULATION PROCEDURE

Details of the proposed correlation between smooth-bar properties and notch rupture behavior may be found in Section III of this report. Calculation steps are summarized here for convenient reference.

Preliminary Calculations:

Determine the distribution of stresses in the three principal directions (axial, tangential, radial) at the plane of the notch. Divide the cross section at the notch into a number of imaginary rings of such a size that the stress at the centroid of any one ring is not too different from the stress at other locations in the ring. Convert to deviator components by subtracting one-third of the sum of the three principal stress components of each ring from each individual component.

The effective stress for any ring now equals the square root of one-half the sum of the squares of the differences between the three pairs of deviator stress components.

Step 1.

Refer to a plot of stress versus creep rate, with separate curves for different fractions of total life expired. Read the effective creep rate corresponding to the effective stress at the centroid of each ring being considered.

For each ring, the component of the creep rate in each principal direction equals three-halves the effective creep rate times the ratio:

$$\frac{\text{deviator stress component in desired direction}}{\text{effective stress of the ring}}$$

Step 2.

Perform subtractions to determine the differences in creep rate between each pair of adjacent rings and for each of the three principal directions.

Step 3.

These differences in component creep rates are next converted into equivalent changes in stress for a time interval chosen small enough that the creep rates do not vary much over the interval. When all stresses involved are below the proportional limit, stress interactions in any direction at the interface of a pair of rings equals the difference in component creep rates found in Step 2, multiplied by the time interval chosen and by twice the shear modulus of elasticity. For each component direction the total stress interaction is distributed inversely as the respective areas of the two rings involved. The magnitude of stresses drops in the ring with the higher creep rate and increases for the ring with the lower creep rate.

Step 4.

For each ring the component deviator stresses are corrected for the stress changes which resulted from the interactions at its two boundaries. The change for the time interval considered is taken as the net result of the stress gain at one interface and the stress decline at the other.

Step 5.

Combine the new values of component deviator stresses for each ring to get the new effective stress at its centroid.

Step 6.

By reference to a plot of stress versus rupture life, estimate the fraction of life used up in each ring at the stress levels present during the time interval just considered.

Step 7.

Knowing the new effective stresses and the cumulative expenditure of life to date, the plot of stress versus creep rate may again be used to find the new effective creep rate for each ring, and the process repeated from Step 1.

TABLE OF CONTENTS

LIST OF TABLES

LIST OF ILLUSTRATIONS

LIST OF ILLUSTRATIONS (cont'd)

LIST OF ILLUSTRATIONS (cont'd)

INTRODUCTION

Stress raisers are a significant factor in the design of most engineering structures. In recent years engineers have made increasing use of rupture tests on notched specimens to evaluate ability of alloys to withstand stress concentrations during high-temperature service. In the usual tests, time to rupture is compared for notched and smooth bars with the same minimum diameter and the same applied axial load. The present investigation was initiated under Air Force Contract No. 18(600)-62 to study factors affecting notch sensitivity in such tests of heat-resistant alloys at elevated temperatures. Special attention was to be given to the significance of stress relaxation by creep and to effects of certain metallurgical variables in rupture tests of notched bars.

Preliminary studies have been presented in a prior Technical Report prepared by the present authors. (See Ref. 1.) Major findings have been integrated into Section I of the present report.

This whole program has been based on the belief that variable response to notches for different materials or for the same material at different temperatures or for differing notch geometry must be closely related to stress-time relationships controlled by creep relaxation. If the residual effective stress can drop quickly enough, life is increased by presence of the notch; if relaxation is slow, a major portion of the total life is quickly expended in areas of high initial stress. In this latter case residual stresses around the notch may eventually fall to quite low values, but by this time only a small fraction of rupture life remains and failure occurs earlier than for a smooth bar with the same nominal stress.

At the onset it was reasoned that a notch introduces nothing inherently new into properties of an alloy, but only changes the stress-strain histories of fibers in the notched bar. If one were to reproduce in a smooth bar the history of effective stress experienced by a fiber of a notched bar, the life of each should be the same. It is not sought here to explain why a smooth-bar rupture specimen behaves as it does. Rather, it is hoped that given the properties of an alloy as ordinarily tested in tension, one might extend these results to other cases where stress conditions are not uniform, but where the initial stress distribution may be estimated.

SECTION I

EXPERIMENTAL RESULTS FOR THREE HEAT-RESISTANT ALLOYS

The proposed method to correlate notched-bar rupture strength with smooth-bar properties required a variety of test results. Besides comparative rupture time for notched and smooth bars, several other types of data were obtained for each condition studied:

1. Short-time tensile properties to permit estimation of initial stress patterns when localized stress concentrations exceed the yield point.

2. Creep curves for each of several constant stresses, supplemented by relaxation data for a number of initial stresses give a measure of stress changes during testing in a notched bar for which the initial stress pattern on loading is known.

3. The proposed correlation requires a method of predicting rupture life in a fiber for which the applied stress varies with time. A suitable answer was sought by conducting tests with smooth bars for one constant stress over part of the run and then changing to a higher or lower constant stress for another portion of the test.

Experimental conditions of temperature, notch geometry, metallurgical condition and stress level have been varied to give widely different degrees of notch strengthening or weakening. For each of the three alloys studied it has been found possible by some means to obtain notched-bar rupture lives both greater and less than for corresponding smooth specimens.

Only part of the notched-bar rupture data were obtained under the present contract since results were already available from another laboratory for bars from the same heats of alloys and with the same conventional heat treatments. (See Ref. 2.)

Materials and Test Conditions

Three typical turbine-blade alloys used in jet engines were tested: a cobalt-base forging alloy (S-816), a chromium-nickel alloy

precipitation hardened with Cb, Ti and Al (Inconel X-550), and a chromium-nickel-cobalt-molybdenum alloy precipitation hardened with Ti and Al (Waspaloy). Chemical compositions were as reported in Table 1 below.

TABLE 1

CHEMICAL COMPOSITIONS OF ALLOYS TESTED

Element	S-816 (Heat 63730)	Waspaloy (Heat 44036)	Inconel X-550 (Heat Y-7180-X)
C	0.38	0.08	0.05
Mn	1.22	0.80	0.73
Si	0.49	0.61	0.28
P	0.012	0.017	--
S	0.018	0.017	0.007
Cr	20.04	18.72	14.97
Ni	19.43	Bal	Bal
Mo	3.98	2.93	--
W	3.93	--	--
Cb	2.89	--	1.03*
Co	43.32	13.44	--
Fe	3.44	1.17	6.59
Al	--	1.29	1.16
Ta	0.85	--	--
Ti	--	2.29	2.5
Cu	--	0.10	0.03

* Cb + Ta

Except for a few notched bars discussed later, all specimens were machined after heat treatment in University of Michigan laboratories. The following conventional heat treatments were used:

S-816	Waspaloy	Inconel X-550
2150°F, 1 hr, W.Q. + 1400°F, 12 hrs, A.C.	1975°F, 4 hrs, A.C. + 1550°F, 4 hrs, A.C. + 1400°F, 16 hrs, A.C.	2150°F, 1 hr, A.C. + 1600°F, 4 hrs, A.C. + 1350°F, 4 hrs, A.C.

All three alloys were tested at a common temperature of 1350°F, with additional tests on Waspaloy at 1500°F. Some studies to determine influence of metallurgical variations on notch properties were conducted on S-816 and on Waspaloy after several non-standard treatments. Most of these latter tests were carried out at 1500°F on specimens treated as follows:

S-816	Waspaloy
2325°F, 1 hr, W.Q. + 13.5% Reduction at 1200°F + 1400°F, 12 hrs, A.C.	1975°F, 4 hrs, A.C. + 15% Reduction at 75°F + 1550°F, 4 hrs, A.C. + 1400°F, 16 hrs, A.C.

All tests were conducted in individual beam-loaded creep-rupture units. Temperatures were controlled to ±3°F. Usual practice was to place a specimen into a cold furnace the night prior to start of the test and to allow the furnace to rise to 100°F below the desired testing temperature. The specimen was brought to the final value and the temperature distribution adjusted over a period of between 2 and 5 hours just before loading.

Comparative Rupture Properties of Smooth and Notched Bars

Stress versus rupture life for smooth and notched bars are shown in Figures 1 through 7 for the six conditions chosen for detailed study. Test points have been distinguished on these plots for differing notch geometry and methods of notch preparation.

S-816 with conventional heat treatment (Fig. 1) appears to be markedly strengthened by notches with a considerable range of root radius. Results seem to be independent of whether the notch was prepared by grinding or turning. Carlson, et al. (Ref. 2) found similar notch strengthening at 1500° and 1600°F. Of the conditions investigated during studies of metallurgical variables, raising the solution temperature of S-816 to 2325°F and then reducing the bars 13.5% by rolling at 1200°F before the 12-hour aging at 1400°F gave much lower ductilities and creep rates than did other treatments. Notch weakening at a test temperature of 1500°F was found for S-816 in this condition. (See Fig. 2.)

Waspaloy with conventional heat treatment was uniformly strengthened at 1500°F by ground notches with root radii between 0.005 and 0.100 inch. (See Fig. 3.) At a test temperature of 1350°F, however, the sharper notches lowered rupture strength over a range of applied stress. The larger notch root radii gave rupture lives equal to or exceeding those for smooth bars at like nominal stress levels. (See Fig. 4.)

Waspaloy specimens cold-rolled between solution and aging treatments were investigated for possible decrease in notch strengths similar to that noted in S-816 studies. Room-temperature rolling to reductions of 5% or 15% between conventional solution and aging treatments lowered the rupture life of Waspaloy at 1500°F below that for specimens treated conventionally. Turned notches with a single notch geometry gave somewhat scattered results, but in this condition both smooth and notched bars appeared to give a common curve of stress versus rupture life. (See Fig. 5.)

Inconel X-550 with conventional heat treatment exhibited a slight strengthening at 1350°F from ground notches at high test stresses. At lower stress levels marked notch weakening set in, but with some indication that at still lower stresses the notched-bar strength might again rise to that of smooth bars. (See Fig. 6.)

Figure 7 shows additional data for bars of Inconel X-550 with a common notch geometry but with the notch prepared in various ways. Under some conditions the method of notching appears to be an important variable in tests of this nature.

Variation of Notched-Bar Rupture Life with Method of Notch Preparation

Under one condition of notch strengthening (S-816 at 1350°F), no difference had been noted between specimens prepared by turning or by grinding. Furthermore, results from different laboratories were in close agreement.

During a further cross check between laboratories a few bars of Inconel X-550 with a ground root of 0.005-inch radius were tested at the University of Michigan for comparison with findings of Carlson, et al. (Ref. 2). Some of the rupture times fell far short of those expected. Possible explanations for this variation in test results include the presence of unknown residual stresses left by the notching operation and structural alteration of the metal as a result of plastic deformation during machining. A special study was begun to investigate this observed spread of data and to seek a method of notch preparation free from extraneous effects introduced from machining operations.

Notches were prepared at different stages of the heat treatment, using three different machining methods:

1. After preliminary rough turning within 0.015 to 0.020 inch of the desired notch diameter, the final notch root was made by a light cut with a formed lathe tool.

2. Notches were rough turned 0.015 to 0.020-inch oversize as above and then rough ground to within about 0.005 inch of the final size. The finish grinding to size was done in light cuts with a hand-dressed wheel. All grinding was with a rather hard wheel turning at quite high speed (Carborundum wheel A80V2BT, 6-inch diameter, running at 5200 RPM). The specimen was rotated counter to the wheel at 1100 RPM. Hand feeding of the grinding wheel was about 0.001 inch per 160 revolutions of the specimen. Afton No. 8 (Tidewater Oil Co.) coolant was used.

3. A notch was first turned to within 0.003 to 0.004 inch of final diameter with a formed lathe tool having a nearly blunt end. The root of the notch was then rounded out and the diameter at the notch was brought to the desired final value using a wire 0.009-0.010 inches diameter and fine lapping compound. (See Fig. 8.) The form lapping required only one or two minutes to remove the desired amount of metal from the notch while the specimen was rotated in a lathe.

Specimens tested had the notches prepared at the following three stages in the heat treatment:

a. After conventional solution and aging treatments

b. After solution, but before aging, to reduce residual stresses

c. Before either solution or aging to remove residual stresses and to minimize metallurgical alteration of the metal due to cold work during machining.

A few bars notched after a complete conventional heat treatment were given stress reliefs at 1500° or 1600°F and then air cooled prior to testing at 1350°F.

All heat-treating operations were conducted in an air atmosphere except for the solution treatment (2150°F, 1 hr, A.C.) of specimens machined in the as-received condition. For these latter samples the solution step was carried out in an atmosphere of commercial-purity helium. As discussed later, this was not completely successful in surface preservation.

Experimental findings are shown in Table 2.

When these data are plotted as in Figure 7, the longest notched-bar rupture lives result for notches turned after conventional heat treatment. Two widely separated curves appear to be necessary for representation of the data for ground notches. For most specimens, grinding gave lives just slightly shorter than did turning, but occasional ground notches resulted in much lower rupture lives than did any other notching method investigated. A shallow lapping after initial turning or grinding lowered rupture life somewhat.

Short stress reliefs at 1500° or 1600°F had little effect on test results, but performing either the entire conventional heat treatment or just the aging portion of this treatment after machining gave a plot of stress versus rupture life approximately midway between the two curves obtained for notches ground after heat treatment.

The observed dispersion of test results for various methods of notch preparation could be attributed to residual stresses left by the notch-forming operation or to structural alteration of the alloy near the notch root due to mechanical working of the metal or changes in precipitation phenomena under the action of residual stresses.

TABLE 2

NOTCHED-BAR RUPTURE TESTS AT 1350°F FOR INCONEL X-550

SPECIMENS WITH DIFFERENT METHODS OF NOTCH PREPARATION

Notch Geometry of All Specimens Unless Otherwise Noted: Shank Diameter: D = 0.600 inch; Diameter of Notch: d = 0.424 inch; Notch Root Radius: r = 0.005 inch; Notch Angle: 60°

Specimen No.	Stress (psi)	Rupture Life (hours)	Remarks
Conventional Heat Treatment + Turn Notch on Lathe			
X-526	60,000	45.0	r = 0.004
X-534	40,000	176.4	r = 0.0055
X-525	35,000	279.3	r = 0.004
X-528	35,000	896.4	
X-527	30,000	160.7	Stress relieved 1500°F, 1 hr, after notching
X-536	40,000	168.6	Stress relieved 1600°F, 20 min, after notching
Conventional Heat Treatment + Grind Notch			
[a]I-13	60,000	30.1	
[a]I-16	50,000	62.8	
[a]I-19	40,000	109.4	
X-535	40,000	110.7	
[a]I-22	35,000	197.4	
X-532	35,000	31.2	
[a]I-40	32,000	697.6	
[a]I-37	30,000	1208.1+	Discontinued
[b]I-53	30,000	130.0	
[b]I-54	30,000	69.6	
X-531	24,520	1343.7	
	35,000	270.9	Stress level raised after 1343.7 hrs.
X-537	40,000	87.5	Stress relieved 1600°F, 20 min, after notching

(continued on following page)

TABLE 2, continued

Specimen No.	Stress (psi)	Rupture Life (hours)	Remarks
	Conventional Heat Treatment + Rough Turn Notch + Lap Notch 0.003 to 0.004 inch on Diameter		
X-551	60,000	28.4	
X-552	50,000	47.0	
X-540	40,000	74.5	Rough Grind before Lapping
X-553	35,000	261.6	
X-554	32,000	622.6	
	As Received + Turn Notch + Conventional Heat Treatment		
X-547	60,000	6.5	r = 0.0055
X-550	50,000	16.0	
X-542	40,000	50.2	
X-544	40,000	60.5	
X-548	35,000	145.0	
X-549	30,000	668.4	
	As Received + Grind Notch + Conventional Heat Treatment		
X-541	40,000	65.1	
X-543	40,000	23.5	r = 0.004
	Conventional Solution Treat Only + Turn Notch + Conventional Aging Treatments		
X-546	40,000	64.4	
X-538	40,000	76.4	
	Conventional Solution Treat Only + Grind Notch + Conventional Aging Treatments		
X-539	40,000	30.7	
X-545	40,000	116.5	r = 0.004

a.) Data of Carlson, et al., Ref. 2.
b.) Specimen machined in same shop as those used by Carlson, et al. (Ref. 2), but tested at Univ. of Mich.

Residual stresses could explain all the results shown in Figure 7. The technical literature (References 3, 4, 5, and 6) reports that residual stresses left after machining and after grinding of flat steel plates may be either tensile or compressive and may reach values near the tensile strength in the direction of machining.

In grinding tests with mild steel (Ref. 4), residual stresses extended to depths of about 0.012 inches to 0.018 inches for grinding cuts ranging from 0.0003 inches to 0.003 inches. (It might be noted that for the 0.005-inch radius notch used in the present program, initial effective stresses from the applied load are greater than the nominal stress only to a depth of about 0.008 inch.) Both the maximum residual stress from machining, found at the ground surface, and the thickness of the stressed layer increased with depth of grind. Lapping of a manganese oil-hardened tool steel was found to leave nearly uniform residual compressive stresses for a depth of 0.000 2 or 0.000 3 inch in one set of tests. (See Ref. 5.)

Other recent studies by Colwell, Sinnott and Tobin (see Ref. 6) indicate that residual stresses in hardened steel may be considered to be made up of compressive ("mechanical") components and tensile ("thermal") components. With short contact times between the workpiece and the cutting edge of the wheel and with continuous efficient cooling, stresses left near the ground surface are compressive, similar to those left by a cutting tool. Slower movement of the work relative to the grinding wheel results in a sharp drop from residual compression to residual tension in most instances. Stresses for still lower relative speeds are somewhat variable according to test conditions, but remain predominately tensile.

With the high speed of rotation of the workpiece and the flood cooling used while grinding notches for the present study and for that of Carlson, MacDonald and Simmons, significant residual compression can be expected near the notch root. However, it has been suggested (Ref. 7) that either a momentary lapse of coolant, even for a few microseconds, or non-uniform feeding with its attendant localized heating by rubbing of the wheel over the work surface could result in lowered compressive stresses or might even cause residual tensile stresses of considerable magnitude.

It is therefore proposed that the "high" values of Figure 7 associated with all turned and most ground specimens reflect residual compressive stresses of variable amounts. The shallow depth of stressed metal removed by lapping still left a state of compression near the notch root. The "abnormally-low" curve for other ground notches corresponds to the occasional occurrence of residual tension through some mechanism such as those discussed above.

If this explanation is accepted, the true curve for rupture life of notched bars free from residual stresses should lie near that obtained with specimens heat treated after notching. Results from these particular tests might be slightly low as a result of any warping of the specimens during cooling after the several heat-treat steps, but difficulty from this source appears not to be serious.

To determine the probable error introduced by warping, eighteen specimens were notched and then given conventional solution and aging treatments. Subsequent examination revealed no measurable distortion for four of the bars and a maximum eccentricity of 0.002-inch from the original axis for any one specimen. The resulting bending moment equals (0.002) (axial load) = (0.002) (a^2S), where a is the radius of the bar at the notch and S is the nominal axial stress. The maximum bending stress, at the radius a, is given by:

$$S_{max.,\ bending} = \frac{\text{(Bending moment, in. lb.)(radius at notch root, in.)}}{\text{(Moment of inertia of notched cross section, In}^4\text{)}}$$

$$= (0.002 \quad a^2S)\,(a) \,/\, (\quad a^4/4) = 0.008\ S/a\ .$$

In the present studies a = 0.212 inch or 0.175 inch for different notched-bar sizes employed, wherefore the maximum stress imposed by warpage of specimens during heat treatment should be less than five percent of the nominal stress in any case.

The mechanism advanced to explain variation in notch behavior on the basis of residual stresses is supported by other data of Table 2. Results for specimens solution treated and then notched before aging lay between the extreme curves for ground notches. Short-time stress relief after notching produced a very slight effect as might be expected for material with low relaxation rates. What effects did result were in the direction expected for reduction of residual stresses. Longer times of stress relief were not tried to avoid serious altering of the basic material properties. A single smooth specimen tested at 40,000 psi after one hour of stress relief at 1500°F gave a rupture life of 765.8 hours compared with a value of 550 hours read from Figure 6 for bars with conventional heat treatment only, which indicates that the stress relief did not reduce life.

The relatively low creep and relaxation rates for Inconel X-550 might be expected to limit the extent of stress relief during reasonable time periods. In contrast, S-816 at 1350°F has quite low relaxation strength and should be capable of eliminating the major portion of any residual machining stresses during temperature adjustment prior to loading, regardless of notching procedure. This may explain why not a single abnormally low point was reported by Carlson, et al., for this alloy, while no fewer than seven such low values can be spotted for tests with Inconel X-550, covering a temperature range from 1350° to 1600°F. (See Ref. 2.) Reference 2 also shows one very low notched-bar point for Waspaloy at 1350°F, at which temperature that alloy also has low relaxation rates, as shown in following pages.

Metallographic Examination of Notches Prepared by Different Methods

Metallographic examination of specimens notched before heat treatment indicated some surface alteration and preferred grain orientation resulted from the treatment. With the information at hand it is impossible to say to what extent these factors affected rupture results reported above for notches prepared by different methods.

Recrystallization of the worked metal in the vicinity of notches given conventional heat treatments after machining tended to result in columnar grains with their long boundaries normal to the machined surface. This tendency was most pronounced in the case of turned notches. Figure 9 (a) shows a particularly prominent example found in one turned specimen, with columnar grains extending inward to a depth of about 0.020 inch. For notches lapped or ground before solution and aging treatments, grains were much more equiaxed, but some indications were found of a possible tendency for grain boundaries to orient perpendicular to the machined surface. Figure 9 (b) illustrated the structure for a notch ground before heat treatment.

These above specimens all showed shallow surface alteration, with grain-boundary oxide penetration to 0.0002 inch or less. (See Fig. 9 (c).) In some of the specimens examined, material within about 0.0005 inch of the surface varied slightly in appearance from the alloy in the rest of the bar, indicating possible alloy depletion from a shallow surface layer during heat treatment.

Machining the notch between conventional solution and aging steps resulted in twinning to a depth of about 0.010 inch along the surface of a ground notch (Fig. 9 (d)) and slightly deeper for a notch prepared by turning. These crude observations should indicate approximate depths to which deformed metal was present after notch preparation and support the hypothesis that residual-stress effects from mechanical working during notching might be expected to be greater for turned notches than for ground or lapped notches.

Relaxation Properties of Alloys Studied and Qualitative Comparison with Notch Sensitivity

Relaxation as used here means replacement of elastic strains by the plastic strain of creep, with consequent reduction in stress. For continuous reduction of the applied load, so as to keep the total strain constant, relaxation may be shown as a smooth curve of residual stress versus time. In the present investigation stress reduction was performed in finite steps. (See Fig. 10.) The specimen was loaded to the highest

values (S_1 at Point A) and the strain reading noted. Creep was then allowed to occur (A-B) until such a time that removal of a weight would return the specimen to its original length (Point C) but at a lower stress (S_2). When a large number of small equal weights are used, the resulting step-wise curve of residual stress versus time approaches the smooth curve corresponding to continuous unloading.

Figure 11 shows actual data from a relaxation test at 1500°F for Waspaloy with an initial stress of 30,060 psi. Stress reduction was by steps of about 2,980 psi. When the specimen was first loaded to 30,060 psi, the total strain at that moment was arbitrarily called zero, and all strains in Figure 11 represent differences from this initial value. Creep was allowed to occur at the constant initial stress until the differential strain reached a value equivalent to the elastic strain from 2,980 psi. Removal of one weight then returned the specimen to its initial strain. Creep was now continued at the new stress level (27,080 psi) until removal of a second weight would again return the specimen to its original total strain.

At the low stresses near the end of the relaxation tests run for this program, it was observed that the instantaneous elastic recovery upon reduction of the applied stress was followed by further contraction of the test specimen over a substantial time period before the bar once again elongated. These secondary recovery periods were included as part of the relaxation times between successive stress levels.

The experimentally-determined relaxation characteristics are shown separately in Figures 12 through 17 for the six conditions used in the notch-sensitivity studies. All six figures are presented to the same scale for easy comparison. Time has been plotted on a hyperbolic sine scale so that the curves can be shown from zero time. Up to one hour this scale is nearly linear, while at times beyond 10 hours it is nearly identical with the logarithmic scale.

On each set of curves the stresses corresponding to rupture in 10 hours and 1,000 hours have been indicated. The times required at 1350°F for smooth bars of S-816, Waspaloy, and Inconel X-550 to relax from their respective stresses for rupture in 10 hours to the 1000-hour rupture stress levels are approximately 0.5, 20, and 150 hours respectively. S-816 with the short relaxation time corresponds to uniform strengthening by all notches studied, the intermediate rate of relaxation of Waspaloy corresponds to the case where some notches increase and others shorten rupture life, while the slow relaxation of Inconel X-550 agrees with severe notch weakening for nearly all notches.

Moderate notch embrittlement at 1500°F of S-816 when rolled after solution treatment at 2325°F is accompanied by a tenfold increase in the time for relaxation from the 10-hour to the 1000-hour rupture stress compared with the time at 1350°F for S-816 with conventional heat treatment. (See Figs. 12 and 13.)

At 1500°F, mild notch strengthening of Waspaloy with standard heat treatment corresponds to a relaxation time of about 5 hours between the 10-hour and 1000-hour rupture stress levels. The same alloy cold rolled between conventional solution and aging steps has a slightly lower relaxation rate and shows little or no notch strengthening.

These several comparisons demonstrate a definite qualitative agreement between notch strengthening or weakening and the rate of stress relaxation under creep conditions. One purpose of this investigation is to see whether the agreement noted can be made quantitative for a range of test conditions.

Addibility of Rupture-Life Fractions

Under the influence of relaxation, fibers in a notched specimen undergo stress changes during a rupture test. The technical literature (Refs. 8 and 9) offers little in the way of experimental findings on suitable means of predicting rupture life under unsteady-stress conditions.

Reference 1 presented test data for rupture tests in which one constant stress was maintained for a portion of the run and then the stress level was changed to a different value for another portion of the test. Though some individual tests gave deviant results, it was concluded that for variable-stress tests at conditions studied the portion of life used up during a period of time at any particular stress equals the fraction:

$$\frac{\text{Actual time at the given stress}}{\text{Rupture life for that stress}} .$$

A Relationship between Creep and Relaxation Properties

If the above simple law holds for the range of stresses involved in a relaxation test, then it should be possible to predict relaxation characteristics directly from a family of creep curves. To permit comparison between relaxation and creep, creep curves have been obtained (Fig. 18) for the same stress levels as were present in one relaxation test from 60,050 psi for Inconel X-550 at 1350°F. Stress decrements in the latter test averaged 3,140 psi, equivalent to an elastic strain of 0.00013 inches/inch. Experimental results are listed in Table 3.

TABLE 3

EXPERIMENTAL DATA FOR RELAXATION OF INCONEL X-550

AT 1350°F FROM AN INITIAL STRESS OF 60,050 PSI

Stress Level (psi)	Time at Stress Level for 0.000 13 in/in Creep Corresponding to 3,140 psi Stress Change (hrs)	Cumulative Time by End of Given Stress Period (hours)
60,050	0.37	0.37
56,820	1.16	1.53
53,680	3.95	5.5
50,530	9.6	15.1
47,410	19.9	35
44,300	31	66
41,190	49	115
38,060	83	198
34,910	123	321
(31,790)		

The corresponding points can now be estimated from creep data, assuming addibility of life fractions. The first interval (0.37 hr) will be taken directly from the initial portion of the relaxation test at constant stress of 60,050 psi. At this stress the rupture life (from Fig. 6) is 30 hours so that the fraction of life consumed was 0.37/30 = 1.23%. If the stress is now reduced until the total strain is returned to the initial value, the new stress level is 56,820 psi. At this new level the rupture life is 55 hours. The 1.23% of life expired to date corresponds to (0.0123)(55) = 0.68 hours. Starting at 0.68 hours on the creep curve of Fig. 18 for 56,820 psi, a creep increment of 0.000 13 inches/inch would end at 1.5 hours, giving a time interval of 1.5 - 0.68 = 0.8 hours. During this second time interval the fraction of life used is 0.8/55 = 1.46%, making the cumulative fraction of life expired 1.23 + 1.46 = 2.7%.

The time coordinate at the start of the third time interval is found from the total life expenditure to date and the rupture life at 53,680 psi: (0.027)(104 hr) = 2.8 hr. Starting at this point, a creep strain of 0.000 13 in/in is reached at 7.0 hours, according to the 53,680 psi creep curve of Figure 18. The third time interval is thus 4.2 hours, making the total relaxation time from 60,050 to 50,530 psi

equal to 1.2 + 4.2 = 5.4 hours. The fraction of life used at this new stress is determined and the process repeated.

Complete calculations to a final stress of 31,790 psi are summarized in Table 4. (This table differs somewhat from the corresponding one in Appendix I of Reference 1, since a long-time rupture test completed after that report resulted in a slight relocation of the stress-rupture life curve for Inconel X-550 at 1350°F.)

Agreement between experimental and calculated relaxation characteristics appears sufficiently close to permit the direct use of creep data in correlations involving relaxation of initial stress concentrations. This has the advantage that creep tests are easier to perform than relaxation tests and creep data are generally more available than are relaxation data.

Variation of Creep Rates with Stress and with Percentage of Life Expired

Creep curves for S-816 and Inconel X-550 at 1350°F and for Waspaloy at 1500°F were included in Reference 1. Similar curves are shown in Fig. 19 for Waspaloy at 1350°F after conventional heat treatment. Rupture data for these latter tests were as follows:

RUPTURE PROPERTIES OF WASPALOY AT 1350°F

Stress (psi)	Rupture Life (hrs)	[a]Elongation (%)	Reduction of Area (%)
90,000	0.29	2.5	8.5
80,000	1.4	3.	7.
70,000	7.4	4.	8.
40,000	512.1	3.	6.5

a.) Based on gauge length of 2.1 inches.

In Figure 4 these results were combined with the following data obtained for this same heat by Carlson, et al. (Ref. 2).

Stress (psi)	Rupture Life (hrs)	Elongation (%)	Reduction of Area (%)
60,000	10.6	2.6	5.3
55,000	56.6	3.0	5.8
50,000	161.4	5.2	6.7
45,000	256.1	5.3	6.9
35,000	1201.6 + (discontinued)	--	--

TABLE 4

CALCULATION OF RELAXATION FOR INCONEL X-550

AT 1350°F FROM CREEP DATA, ASSUMING ADDITIVITY OF LIFE FRACTIONS

Creep Stress (psi)	Rupture Life at Given Stress (hrs)	[a]Time Coordinate at Start of Given Creep Period (hrs)	Time for Creep of 0.00013 in/in at Given Stress (hrs)	Fraction of Life Expended at Given Stress	Cumulative Fraction of Life Expended	Cumulative Time of Creep Periods(hr)
60,050	30	0	0.37	0.37/30 = 0.0123	0.0123	0.37
56,820	55	(0.0123)(55) = 0.68	1.5 - 0.68 = 0.8	0.8 /55 = 0.0146	0.027	1.2
53,680	104	(0.027)(104) = 2.8	7.0 - 2.8 = 4.2	4.2 /104 = 0.040	0.067	5.4
50,530	145	(0.067)(145) = 9.7	20.8 - 9.7 = 11.9	11.1/145 = 0.077	0.144	16.5
47,410	190	(0.144)(190) = 27.4	44.0 - 27.4 = 16.6	16.6/190 = 0.087	0.221	33.1
44,300	310	(0.22)(310) = 68.3	87.5 - 68.3 = 19.2	19.2/310 = 0.062	0.283	52.3
41,190	470	(0.283)(470) = 133	186.8 - 133 = 53.8	53.8/470 = 0.115	0.398	106.1
38,060	740	(0.398)(740) = 295	351 - 295 = 56	56 /740 = 0.076	0.474	162
34,910	1500	(0.474)(1500)= 710	[b](186)			348
(31,790)						

a.) Calculated as the product of the rupture life at the given stress in a conventional constant-stress rupture test and the total fraction of life already expended at previous stress levels in the step-down test.

b.) Estimated from plot of stress versus creep rate at 50% life expended (Fig. 27).

Short-time tensile characteristics determined from the loading curve of the specimen allowed to creep at 90,000 psi are shown in Figure 20.

The calculation methods proposed in the following section make use of variations in creep rate for different fibers in a notched bar. The creep rate in any particular fiber is affected not only by the stress level existing, but also by the stage of creep present. At early portions of the specimen's life, all fibers experience a decreasing rate of creep at constant stress, whereas the creep rate accelerates for any steady stress level as the end of the fiber's life is approached.

To get the data in convenient form for the intended use, cross plots were prepared showing creep rate as a function of stress, but with the percent of life expired as a parameter. (See Figures 21 through 27.)

Most data points for these plots were obtained by measuring the slopes of creep curves at times corresponding to fixed fractions of the rupture life for the stress concerned. A few supplementary values were obtained from multiple-stress creep tests and relaxation tests.

The general character of the resultant plots is quite similar, with slight divergence of curves at lower stresses in the initial or decreasing rate period of creep, a period of essentially constant creep rate at each stress, and finally an increasing rate period with curves nearly parallel to that of the minimum rate curve on the semi-log coordinates used. Exact placement of individual curves is open to argument in some cases. However, the range of creep rates involved is so wide that considerable latitude is possible without serious effects on the proposed calculations.

For S-816 at 1350°F with conventional heat treatment (Figures 21 and 22) separate curves show the greater initial rate of creep obtained when specimens were prestrained by overloading at temperature just prior to start of the creep test. This effect of prior strain on creep and relaxation rates was shown previously (Ref. 1) to be quite noticeable in the case of S-816, but did not appreciably alter relaxation properties in limited tests with Waspaloy at 1500°F and Inconel X-550 at 1350°F.

SECTION II

ANALYSIS OF CHANGES IN STRESS DISTRIBUTION FOR A NOTCHED BAR DURING LOADING AND DURING CREEP TO RUPTURE

This investigation has been based on the belief that variable response of materials to notches at elevated temperatures must be closely related to initial stress concentrations and their change with time, as controlled by creep and relaxation.

The following treatment was developed around this basic consideration. A former colleague, Dr. Paul Chenea, proposed the idea of following changes of the stress levels in representative fibers in the plane of a notch and at various radii from the axis of the bar as relaxation reduced initial stress concentrations. Professor Chenea left the University of Michigan before all details of the calculations had been settled, but his suggestions and criticisms have been most helpful.

Distribution of Stresses in Notched Bars Loaded Elastically

Consideration is limited here to deep notches with notch root radii between 0.005 and 0.100 inches. The diameter at the notch (0.424 inch in most specimens studied) has been chosen to give a notch cross section half that of the shank.

The theory of elastic stresses around deep circumferential notches is covered by Neuber in his widely-adopted treatment. (See Ref. 10.) In his analysis, Neuber assumes the notch to be a hyperboloid of revolution, but he points out that only the curvature at the base of the notch exerts maximum effect on stress concentrations, so that the results may be applied with little error to notches used in the present investigation.

In the plane of the notch, the stress components in the axial, tangential and radial directions for a bar under axial tension may be expressed:

$$S_a = \frac{1}{\cos v}\left\{ B - C(1+\alpha) \right\} + \frac{1}{\cos^3 v}\left\{ -A + B + C\cos^2 v \right\} \qquad (1)$$

$$S_t = \frac{1}{\cos^2 v}\left\{ A\,\frac{\cos v}{1+\cos v} - B\cos v + C(\alpha - 2)(\cos v) \right\} \qquad (2)$$

$$S_r = \frac{1}{\cos v}\left\{\frac{-A}{1+\cos v} + (\alpha - 1)(C)\right\} + \frac{1}{\cos^3 v}\left\{A - B - C\cos^2 v\right\} \qquad (3)$$

(These expressions follow immediately from Equations { 50 } on page 86 of Reference 10 at $u = 0$, so that h^2 of Neuber's equations equals $\cos^2 v$).

In these equations the parameter v is related to radial distance x by $x = \sin v$, and the constant α to Poisson's ratio (1/m) by $\alpha = 2(1 - 1/m)$. For the alloys and temperatures in this program 1/m is about 0.3 or 0.32 for elastic conditions. A value of 1.4 will be used for α. Constants A, B and C are functions of the nominal axial stress p = (axial load)/(πa^2), where a is the radius of the bar at the notch; i.e., 0.212 inch for the specimen adopted for most notched bars in this program. The ratio of this minimum radius to the root radius of curvature r of the notch is used by Neuber to define a new parameter v_0, such that $a/r = \tan^2 v_0$, or

$$\cos v_0 = 1 / \sqrt{(a/r) + 1}$$

$$\sin v_0 = \sqrt{(a/r) / (a/r + 1)} \quad .$$

A, B, and C may now be ~~defined~~ expressed in terms of the above parameters:

$$\left.\begin{aligned} C &= (-p/2)\,\frac{1 + \cos v_0}{1 + (2 - \alpha)(\cos v_0) + \cos^2 v_0} \\ A &= (\alpha - 1)(1 + \cos v_0)\,C \\ B &= A - C\cos^2 v_0 \end{aligned}\right\} \qquad (4)$$

Introducing ~~1.4~~ for α and simplifying:

$$\left.\begin{aligned} S_a &= \{(B - 1.4C) / \cos v\} + \{(B-A)/\cos^3 v\} \\ S_t &= \{-(B + 0.6C) / \cos v\} + \{A/(\cos^2 v + \cos v)\} \\ S_r &= \{-A/(\cos^2 v + \cos v)\} - \{0.6C / \cos v\} + \{(A-B)/\cos^3 v)\} \end{aligned}\right\} \qquad (5)$$

$$\sin v = (x/a)\sqrt{(a/r) / (a/r + 1)}$$

These equations will be applied to the specific example of a notched specimen with radius of curvature r = 0.005 inch at the notch root and with a = 0.212 inch.

$$a/r = 0.212 / 0.005 = 42.4$$

$$\cos^2 v_0 = 1/(a/r + 1) = 1/43.4 = 0.02305$$

$$\cos v_0 = 0.1519$$

$$\sin v_0 = \sqrt{(a/r)/(a/r + 1)} = \sqrt{42.4/43.4} = 0.9884$$

$$C = (-p/2)\frac{1 + \cos v_0}{1 + (2 - \alpha)(\cos v_0) + (\cos^2 v_0)}$$

$$= (-p/2)\frac{1.1519}{1 + (0.6)(0.1519) + 0.02305} = -0.517\,p\,.$$

$$A = (\alpha - 1)(1 + \cos v_0)\,C = (0.4)(1.1519)(-0.517\,p) = -0.2385\,p$$

$$B = A - C\cos^2 v_0 = -0.2385\,p + (0.517\,p)(0.02305) = -0.2266\,p$$

For a radial distance x equal to half of a,

$$\sin v = (x/a)(\sin v_0) = 0.9884/2 = 0.4942$$

$$\cos v = 0.8694$$

$$\cos^3 v = 0.657$$

The corresponding axial stress component is found to be:

$$S_a = \frac{B - 1.4C}{\cos v} + \frac{B - A}{\cos^3 v}$$

$$= p\left(\frac{-0.2266 + (1.4)(0.517)}{0.8694} + \frac{-0.2266 + 0.2385}{0.657}\right)$$

$$= 0.593\,p.$$

Calculations for the other principal stresses and for other radial distances can be performed in like fashion. Results of such calculations for notch root radii of 0.005 and 0.040 inches are plotted in Figure 28, with the abscissas expressed in terms of areas instead of radii. The point found above for a radius equal to a/2 corresponds to a location at 0.25 of the total cross section out from the axis of the specimen. In addition to the three stress components, the "effective" stress equivalent to their combined effect in causing creep is also shown. The significance of the effective stress will be discussed more fully in a later section.

The most salient aspect of Figure 28 is the localization of severe stress concentration close to the surface of the sharp notch, while stress levels over most of the notched cross section are considerably below the nominal axial stress applied. With this in mind, the cross section of the notched bar will be imagined for calculation purposes to consist of nine concentric rings, but with four of these rings covering the outside ten percent of the area and the innermost ring equal to half the total section. These rings have been indicated on Figure 28 and are repeated on Figure 29 to show radial location of the centroids of the several rings.

General Behavior of Metals During Plastic Flow

When a small axial load is placed on a notched bar with 0.005-inch radius of curvature at the root and 0.424-inch specimen diameter at the notch, Neuber's analysis for an ideal elastic material indicates an axial stress component slightly more than six times the nominal stress for the metal nearest the notch root. The ratio of this maximum theoretical axial stress to the nominal axial stress (load/cross section at the notch) is defined as the theoretical stress concentration factor and is commonly designated by the symbol K_t. In reference 10, α'_k is used to represent this term.

For the same conditions and location considered in the preceding paragraph the tangential stress (in the circumferential or hoop direction) is about twice the nominal axial stress. One may inquire as to how high the tensile load on the notched specimen may be raised before the most-highly stressed fiber will yield under the combined effect of the stress components, and how fast the metal will creep under complex stressing. The general plastic behavior of metals at room temperature is treated by Hill. (See Ref. 11.) There is no reason immediately apparent why his mathematical development should not remain valid at elevated temperatures for changes occurring so rapidly that creep effects are relatively small, provided the necessary physical constants are evaluated at the temperature under consideration. The following observations are taken from Hill's treatment:

1. By experiment, the extent of yielding is but little affected by a moderate superimposed hydrostatic pressure. From this observation it may be reasoned that the component of plastic strain in a given direction

depends not on the magnitude of total stress, but rather on the "deviator" stress in the given direction. This deviator stress (S'_{ij}) is defined as the component of total stress less the arithmetical average of the three principal stresses.

2. The start of yielding appears to depend only on differences between individual principal stresses ($S_1 > S_2 > S_3$). For ductile materials many correlations seem to indicate the following combination of individual stresses as giving a suitable measure of the effective stress ($\overline{S}$) at onset of yielding:

$$2(\overline{S})^2 = (S_1 - S_2)^2 + (S_2 - S_3)^2 + (S_1 - S_3)^2 \qquad (6)$$

In pure tension the value of $\overline{S}$ is simply the axial stress S_1 .

A similar yield criterion in terms of strains can be written:

$$(9/2)(\overline{e})^2 = (e_1 - e_2)^2 + (e_2 - e_3)^2 + (e_1 - e_3)^2 \quad , \qquad (7)$$

where $\overline{e}$ is the axial strain for pure tension and e_1 , e_2 , e_3 are the three principal strains. (Some authors prefer to use the octahedral shear stress and strain, given respectively by $\frac{\overline{S}\sqrt{2}}{3}$ and $\overline{e}\sqrt{2}$).

3. When an increment of plastic strain occurs, the directions of the principal components of this strain coincide with the axes of the total principal stresses existing at that moment, independent of the direction of the added increment of stress. Moreover, the magnitude of plastic strain increments depend on the existing total stresses and not on the stress increment. As a consequence, the plastic-strain history must be followed in a step-wise manner. After each small plastic deformation the new stress pattern is determined. Then the strains may be evaluated for the next stress addition.

The incremental plastic strain (de^p_{ij}) in any direction is related to the incremental effective strain ($\overline{de^p}$) by the following relationship developed on page 39 of Reference 11:

$$de^p_{ij} = \overline{de^p}\ (3/2)(S'_{ij}/\overline{S}) \quad . \qquad (8)$$

4. If an element "unloads", that is, if the effective stress in a fiber decreases, all changes follow the laws of elasticity until such time as the effective stress is again raised to the value from which unloading began.

Application of Plasticity Correlations to Creep and Rupture

The usual methods of handling plastic flow at room temperature seem to be adequate to correlate creep rates under triaxial loading provided an experimental relation is available between stress and creep rate for the state of strain present. Johnson (Ref. 13) compared creep rates of magnesium at 20°C for flat plates pulled in two directions and for combined tension-torsion runs in thin tubes. The two systems were designed to give like values of effective stress, but with the principal stress components in the two cases differing by a constant value of hydrostatic stress. Creep rates were observed to be the same for these two quite different stress patterns. For tests on thin cylinders of four alloys at two or three temperatures each, a plot of octahedral stress versus octahedral strain gave common curves for pure shear, pure tension and variable ratios of shear and tension.

Similar good agreement between theory and experiment was found by Soderberg (Ref. 14) for thin steel cylinders under internal pressure when creep components were compared with corresponding deviator stresses.

The situation is less clear with respect to rupture under combined stresses at creep conditions. From short-time fracture tests on an aluminum alloy in combined tension and torsion, Johnson and Frost (Ref. 15) concluded: "...the criterion appears to be between the octahedral stress and the maximum shear stress, and is certainly not a direct function of the maximum principal stress". But incomplete tests on 0.5% Mo steel and on copper indicated the criterion of fracture might be the maximum principal (tensile) stress of the system imposed.

Proposed Step-Wise Treatment of the Creep-Relaxation Process

When a notched bar is held under constant load at elevated temperature, complex changes in stress and strain throughout the bar may be expected, with gradual leveling of initial stress gradients. In the actual bar the stress levels will vary smoothly from point to point without discontinuities, but to facilitate calculations the cross section will be divided into a sufficient number of concentric rings such that conditions at the centroid of any given ring are quite representative of that entire ring. Further, the actual continuous change in stress pattern will be replaced by an equivalent series of time intervals over each of which the creep rate and stress in a given fiber may be considered nearly constant.

Immediately on loading, a fiber in the notched bar has a unique creep rate determined by the initial effective stress and effective strain. The corresponding creep rates in the three principal directions may then be calculated from a modification of Equation (8):

$$\dot{e}_i^p = \dot{\bar{e}}^p \, (3/2)(S_i' / \bar{S}) \quad . \tag{9}$$

(The dot over a symbol represents "rate", a prime indicates a deviator component, and a bar over a symbol refers to effective stress or strain.)

The component of plastic strain in any direction may result in elongation (creep) of the body, but it could also replace initial elastic strain, with resultant drop in the stress level of the fiber (relaxation). How the total plastic deformation splits between creep and relaxation depends on the extent of stress gradients in the structure.

In a conventional tensile creep bar, where all fibers are subjected to the same stresses until necking occurs, the body can creep as a unit with no reaction of one fiber on another. Such is not the case, however, in a notched bar where the stresses vary continuously from one fiber to the next.

Consider three parallel bands with axial stresses $S_1 > S_2 > S_3$ at their respective centroids. Corresponding axial creep rates, if each band were separate from its neighbors, would be $C_1 > C_2 > C_3$. For continuity to be maintained between filaments, the same total deformation must exist on the two sides of the common interface. This does not say that the deformations at the two edges of a particular band will be the same. The creep rate at different points across any such band in a notched bar will deviate slightly from the rate at its centroid, but this latter value should be quite representative if the band chosen is not too wide.

When band (1) has a total creep in excess of band (2), the difference in plastic strain must be made up by elastic strains in the two bands so long as the fibers of (2) do not become stressed above their yield point. This elastic interaction gives a stress reduction (or relaxation) in band (1) and a stress rise in (2). The absolute values of these two elastic stress changes will be distributed inversely as the areas of the two bands concerned.

Simultaneously, the elastic stress in band (2) is relaxing and that in (3) increasing due to a similar interaction at the 2-3 interface. The net stress change for band (2) can be taken as the difference between the gain from (1) and the loss to (3).

Using this analysis, the physical requirement of constant total axial load in a notched-bar test is automatically met since each time one band drops a certain portion of the axial load by relaxation, a neighbor picks up exactly the same amount of load. The procedure can be applied in turn to strain rates and stresses in all three principal directions.

On occasion the lower-stressed of two adjacent fibers will be above the elastic limit. In this event the stress interaction between the two bands will be reduced considerably below that for the pure elastic case. The load gain of one band will still be set equal to the

load loss of the other, but the stress-strain relationships for the ring with rising stress level must be determined from the short-time tensile curve at the existing stress level.

Applying this approach to concentric rings in the plane of a circumferential notch, analysis will start with the two outermost rings and proceed inward toward the axis. The drop in load for each by relaxation and the gain in load by shift from its neighbor is found for each ring for the same short time interval. When all changes are known, the new stress levels in each ring are calculated and the process repeated.

During the first time interval considered, each ring has been subjected to some average stress level for the given length of time, so that a fraction of the total rupture life of each ring has been used up. Initial correlation attempts will assume that the portion of rupture life consumed during any interval equals the fraction:

$$\frac{\text{actual time at a given effective stress}}{\text{rupture time at this effective stress.}}$$

When the entire life has expired for any one fiber, failure of the notch bar will be considered to have initiated and rupture should be imminent.

Part of the data of Johnson and Frost referred to above indicates that rupture life depends on the largest single stress, that is, on the axial component in the present case. If the analysis indicated here is correct, the axial component should not fall below the nominal stress, at least for a major portion of the test. This, plus the fact that other data refute the role of the largest principal stress as controlling rupture, was the reason for using the effective stress in the above fraction.

SECTION III

CALCULATIONS ILLUSTRATING THE PROPOSED CORRELATION METHOD

For the notches tested in this program the region of stress concentration occupies approximately the outer one tenth of the notched cross section. The notched section was imagined to be divided into a central core covering one half of the total area, surrounded by four rings each with one tenth of the area, plus four outer rings each with one fortieth of the total area. These rings are designated consecutively by numbers from one to nine. (See Fig. 29.)

Consider a Waspaloy specimen with 0.100-inch root radius loaded to a nominal stress p = 25,000 psi at 1500°F. Applying equation (5) for these conditions, the ratios of the principal stress components and of the effective stress to the nominal value are found to be as follows for the centroids of the rings considered in Figure 29:

Ring No.	Axial Stress Ratio (S_a/p)	Tangential Stress Ratio (S_t/p)	Radial Stress Ratio (S_r/p)	Effective Stress Ratio ($\bar{S}/p$)
9 (outermost)	1.72	0.42	0.02	1.54
8	1.64	0.415	0.055	1.44
7	1.56	0.41	0.09	1.34
6	1.50	0.40	0.11	1.27
5	1.27	0.38	0.19	1.00
4	1.19	0.365	0.21	0.91
3	1.06	0.35	0.25	0.77
2	0.97	0.335	0.265	0.67
1	0.79	0.30	0.28	0.50

Even for the most-highly stressed ring (number 9), the effective stress at the centroid under 25,000 psi nominal axial stress is only (1.54)(25,000 psi) = 38,500 psi. This is well below the elastic limit of about 50,000 psi indicated for this alloy on Fig. 30, reproduced from Fig. 20 of Ref. 1. Initial stress components for all rings can consequently be found immediately by taking the product of the nominal stress and the elastic stress ratios listed above. (When stresses for fibers near the notch root exceed the elastic limit during loading, the initial stress distribution can be obtained by approximate methods outlined in Appendix I.)

Initial stress components for the centroids of the several rings under study may now be tabulated:

Ring No.	Axial Stress, S_a (psi)	Tangential Stress, S_t (psi)	Radial Stress, S_r (psi)
9	43,100	10,600	530
8	41,000	10,400	1380
7	38,900	10,200	2250
6	37,500	10,000	2800
5	31,800	9,450	4670
4	29,700	9,100	5350
3	26,600	8,750	6150
2	24,200	8,400	6630
1	19,800	7,550	7100

These values may be converted to deviator components using relationships previously cited:

$$S'_a = S_a - 1/3\ (S_a + S_t + S_r)$$

$$S'_t = S_t - 1/3\ (S_a + S_t + S_r)$$

$$S'_r = S_r - 1/3\ (S_a + S_t + S_r)$$

Results of these calculations are listed in Table 5, along with levels of effective stress for each ring.

TABLE 5

INITIAL CONDITIONS AT THE CENTROIDS OF THE SEVERAL RINGS CONSIDERED IN THE ANALYSIS OF A NOTCHED BAR OF WASPALOY LOADED TO 25,000 PSI AT 1500°F. (NOTCH ROOT RADIUS 0.100 INCH)

Ring No.	Deviator Stress Components (psi) S'_a	S'_t	S'_r	Effective Stress (psi) $\bar{S}$	Creep Rate (in./in./hr.) $\dot{e}^p$
9	25,000	-7,500	-17,550	38,500	0.00180
8	23,400	-7,200	-16,200	36,000	0.00125
7	21,800	-6,900	-14,900	33,400	0.00084
6	20,700	-6,800	-14,000	31,700	0.00063
5	16,500	-5,900	-10,600	25,000	0.00022
4	15,000	-5,600	-9,400	22,700	0.00014
3	12,800	-5,100	-7,700	19,300	0.000078
2	11,100	-4,700	-6,450	16,800	0.000048
1	8,300	-3,900	-4,400	12,500	0.000020

During the experimental program on this alloy, complete smooth-bar creep curves were obtained for a range of stress levels. These were cross plotted to show stress versus creep rate for different percentages of total life expired. Thus, one curve gave initial creep rates for zero % life expired; a second showed minimum creep rates (approximately 5 to 15% of total life expired). Other curves showed creep rates for times equal to 0.4, 0.6, and 0.8 of the rupture lives at the several creep stresses employed. (See Fig. 25.)

From these plots the effective creep rate $\dot{\bar{\epsilon}}^p$ can be found corresponding to the effective stress $\bar{S}$ for each ring. The initial creep rate for each ring has been added to Table 5. Values from that tabulation will now be used to illustrate the steps in a typical calculation cycle.

Step 1.

For any given ring the deviator components of creep are distributed in proportion to the deviator stresses:

$$\dot{e}_i' = (3/2)(\dot{\bar{\epsilon}}^p)(S_i'/\bar{S}) \ .$$

As an example, for Ring 9:

$\dot{e}_a'$ = (3/2)(0.0018 in/in/hr)(25,000/38,500) = 0.00175 in/in/hr.

$\dot{e}_t'$ = (3/2)(0.0018 in/in/hr)(-7,500/38,500) = -0.000525 in/in/hr.

$\dot{e}_r'$ = (3/2)(0.0018 in/in/hr)(-17,550/38,500) = -0.00123 in/in/hr.

Similarly, for Ring 8:

$\dot{e}_a'$ = (3/2)(0.00125 in/in/hr)(23,400/36,000) = 0.00122 in/in/hr.

$\dot{e}_t'$ = (3/2)(0.00125 in/in/hr)(-7,200/36,000 = -0.000375 in/in/hr.

$\dot{e}_r'$ = (3/2)(0.00125 in/in/hr)(-16,200/36,000 = -0.00084 in/in/hr.

and for Ring 7:

$\dot{e}_a'$ = (3/2)(0.00084 in/in/hr)(21,800/33,400) = 0.00082 in/in/hr.

$\dot{e}_t'$ = (3/2)(0.00084 in/in/hr)(-6,900/33,400 = -0.00016 in/in/hr.

$\dot{e}_r'$ = (3/2)(0.00084 in/in/hr)(-14,900/33,400) = -0.00056 in/in/hr.

Step 2.

Perform subtractions for each component and each pair of Rings:

	Component Deviator Creep Rates (in/in/hr)		
Ring No.	$\dot{e}'_a$	$-\dot{e}'_t$	$-\dot{e}'_r$
9	0.00175	0.000525	0.00123
8	0.00122	0.000375	0.00084
9 - 8	0.00053	0.000150	0.00039
8	0.00122	0.000375	0.00084
7	0.00082	0.000160	0.00056
8 - 7	0.00040	0.000215	0.00028

Step 3.

The differential creep-rate components may be converted to stress changes for a time interval chosen small enough that the assumption of constant conditions over the interval is not too far in error:

Stress component change = (psi)

(Difference, between Rings, of component creep rate (in/in/hr))(Time interval (hr))(An area-modulus factor (psi/in/in)) (10)

In relaxation, it may be recalled that plastic creep strains replace equal but opposite elastic strains initially present, so that relaxing fibers exhibit behavior characteristic of both plastic and elastic deformation. In the elastic region the generalized relationship between components of stress and strain may be expressed:

$$S_{ij} = \lambda e_{ii} \delta_{ij} + 2G e_{ij}, \quad (11)$$

where λ is a proportionality constant and G is the shear modulus.

By the assumption of plastic incompressibility inherent to the criterion of yielding and of creep already adopted in this analysis, e_{ii} can be set equal to zero. Therefore changes of principal stresses and strains for relaxation are related by

$$\Delta S_i = 2G \Delta e_i \quad (12)$$

Since differences in deviator components are the same as differences in total components, this same expression relates deviator changes. The factor $2G$ is related to the elastic modulus (E) and Poisson's ratio (1/m) by:

$$2G = E / (1 + 1/m). \quad (13)$$

Available data indicate that (1/m) has a value of about 0.32 within the elastic range for alloys of interest to this program at a test temperature of 1500°F. Incompressibility requires that (1/m) approach 0.5 as a fully-plastic state is reached. However, Neuber (Ref. 10) showed only a small change in elastic stress components for (1/m) between 0.2 and 0.5, and once loading is completed stresses near the notch root decline steadily from their peak values by an elastic redistribution of the stresses. In cases where slight localized plastic straining occurs near the notch root, changes in Poisson's ratio are probably not measureable and have been neglected in the calculations made here.

The distribution of stress changes between a pair of adjacent rings with different creep rates may be seen from consideration of Figure 31, which shows two bands (1) and (2) in simple tension with respective cross sections A_1 and A_2. In a given time interval creep would change the lengths from $\underline{ab}$ to $\underline{ac_1}$ and $\underline{ac_2}$ if the bands could creep independently. The two bands may now be strained amounts δ_1 and δ_2 in opposite directions until the creep-strain difference Δc is "made up" to restore the continuity of the two bands at their interface.

$$\delta_1 + \delta_2 = \Delta c \qquad \{ I \}$$

To preserve the boundary condition of constant total axial load, the load picked up by band (1) must equal that dropped by (2):

$$(\Delta S_1)(A_1) + (\Delta S_2)(A_2) = 0$$

$$\Delta S_2 = -\Delta S_1 (A_1/A_2) \qquad \{ II \}$$

For elastic changes it was shown earlier that $\Delta S_i = 2G\, \Delta e_i = 2G\, \delta_i$. But under some conditions the stress gain by the lower-stressed of a pair of interacting rings may place it into the yield range. In such a situation the deformation required for a given stress change is larger than for the elastic case by the ratio (E/H'), where H' is the slope of the tensile curve at the stress level of the ring being strained plastically.

The higher-stressed ring (number 2 in the present instance) will always be relaxing elastically to lower effective stress level, so that

$$\Delta S_2 = 2G(-\delta_2), \text{ or } \delta_2 = -(1/2G)(\Delta S_2) \qquad \{ III \}$$

For the ring with increasing effective stress:

$$\Delta S_1 = +2G(\delta_1)(H'/E)$$

$$\delta_1 = (\Delta S_1)(1/2G)(E/H') \qquad \{ IV \}$$

Substituting $\{ III \}$ and $\{ IV \}$ into $\{ I \}$:

$$\Delta c = \delta_1 + \delta_2 = \frac{1}{2G} \left\{ (E/H')(\Delta S_1) - \Delta S_2 \right\}$$

Replacing ΔS_2 by its equivalent from {II} :

$$\Delta c = \frac{\Delta S_1}{2G}\left\{\left(\frac{E}{H'}\right)+\left(\frac{A_1}{A_2}\right)\right\} = \frac{\Delta S_1}{2G}\left\{\frac{(E/H')\,A_2 + A_1}{A_2}\right\}$$

Therefore, $$\Delta S_1 = (\Delta c)\left\{\frac{E}{1+(1/m)}\right\}\left\{\frac{A_2}{(E/H')\,A_2 + A_1}\right\}$$

$$\Delta S_2 = (\Delta c)\left\{\frac{-E}{1+(1/m)}\right\}\left\{\frac{A_1}{(E/H')\,A_2 + A_1}\right\}$$

The general area-modulus factors to be introduced into Eq. 10 for the higher-stressed ring (n) and the lower-stressed ring (n-1) of any pair can thus be expressed:

$$\left.\begin{aligned}\text{Area-Modulus Factor})_{\text{ring n}} &= -\left\{\frac{E}{1+(1/m)}\right\}\left\{\frac{H'_{n-1}\,A_{n-1}}{E\,A_n + H'_{n-1}\,A_{n-1}}\right\}\\ \text{Area-Modulus Factor})_{\text{ring n-1}} &= +\left\{\frac{E}{1+(1/m)}\right\}\left\{\frac{H'_{n-1}\,A_n}{E\,A_n + H'_{n-1}\,A_{n-1}}\right\}\end{aligned}\right. \qquad (14)$$

An illustration of the use of this general form of the area-modulus factor is included in Appendix I. For elastic strain distribution between rings of equal area, the factor is numerically equal to G, with opposite signs for the two rings.

At 1500°F Waspaloy has an elastic modulus of 21 x 10^6 psi/in/in, so that

$$G = (1/2)\left(\frac{E}{1+(1/m)}\right) = (1/2)\,(21 \times 10^6/1.32)$$

$$= 7.96 \times 10^6 \text{ psi/in/in.}$$

Using a time interval of 0.3 hour, changes in stress resulting from the interaction between rings (9) and (8) calculated by Eq. 10 would be:

$\Delta S_{a)\ \text{ring 9}}$ = (0.00053 in/in/hr)(0.3hr)(-7.96 x 10^6 psi/in/in) = -1,260 psi

$\Delta S_{a)\ \text{ring 8}}$ = (0.00053 in/in/hr)(0.3hr)(+7.96 x 10^6 psi/in/in) = +1,260 psi

$\Delta S_{t)\ \text{ring 9}}$ = (-0.000150 in/in/hr)(0.3hr)(-7.96 x 10^6 psi/in/in) = +360 psi

$\Delta S_{t)\ \text{ring 8}}$ = (-0.000150 in/in/hr)(0.3hr)(+7.96 x 10^6 psi/in/in) = -360 psi

$\Delta S_{r)\ \text{ring 9}}$ = (-0.00039 in/in/hr)(0.3hr)(-7.96 x 10^6 psi/in/in) = +930 psi

$\Delta S_{r)\ \text{ring 8}}$ = (-0.00039 in/in/hr)(0.3hr)(+7.96 x 10^6 psi/in/in) = -930 psi

The length of time interval was chosen arbitrarily so as to limit the change in any deviator stress component to about 1000 psi. Use of a smaller time interval would more nearly fulfill the condition of essentially-constant creep rate in each ring during the interval, but would increase the number of calculation cycles.

Results of calculations for rings (9) through (7) follow:

Ring No.	Component Deviator Stress Changes in First 0.3 Hour (psi)		
	Axial	Tangential	Radial
(9	-1260	+360	+930
(8	+1260	-360	-930
(8	-950	+510	+670
(7	+950	-510	-670

Step 4.

Correct the component deviator stresses for each ring by the net change resulting from interaction with adjacent rings. During the first 0.3 hour, the axial stress level in ring (9) drops 1260 psi and ring (8) would show a stress rise of 1260 psi by the interaction at the 9-8 interface. Simultaneously the axial stress in ring (8) tends to drop 950 psi at the 8-7 interface. The net effect on ring (8) is +1260 - 950 = +310 psi change in axial deviator stress during the first 0.3 hours. Net changes in the other two principal deviator components and for other rings are obtained in like manner.

Step 5.

Combine the new values of component deviator stresses for each ring to get the new effective stress at the centroid of each ring.

In ring (9) the deviator stress components after 0.3 hour are

S_a = 25,000 - 1,260 = 23,740 psi

S_t = -7,500 + 360 = -7,140 psi

S_r =-17,550 + 930 = -16,620 psi

resulting in an effective stress of 36,600 psi at the end of this initial time interval.

Step 6.

The percent of life expired during the above time interval is found for each ring.

(a). At the initial effective stress of 38,600 psi the rupture life of ring (9) is seen from Fig. 3 to be 12 hours.

(b). At the new effective stress of 36,600 psi at the end of the interval the rupture life is 18 hours.

(c). Applying the findings on addibility of rupture life fractions reported on page 13:

$$\frac{0.3 \text{ hr}}{(12 \text{ hr} + 18 \text{ hr})/2} \quad (100\%) = 2\% \text{ of life expended in ring (9) during the first 0.3 hour of the notched-bar test under study.}$$

Step 7.

Knowing the new effective stresses and the cumulative expenditure of life to date, the new effective creep rate for each ring may be read from the plot of stress versus creep rate and the process repeated for a second interval.

Results of Calculations for Two Particular Cases

As yet the analysis proposed above has been applied to too few test conditions for any conclusions to be drawn as to its validity or usefulness. To date calculations have been completed for two examples with quite different notch behavior:

1. Waspaloy at 1500°F; Nominal stress; 40,000 psi; Notch root radius: 0.100 inch.

2. Inconel X-550 at 1350°F; Nominal stress: 40,000 psi; Notch root radius: 0.005 inch.

For the first set of conditions the experimental ratio (notched-bar life)/(smooth-bar life) was about (3.85)/1, while for the second, the different notch preparation methods represented in Figure 7 give values of this ratio with a ten-fold range from 1/29 to 1/3.1.

Figures 32 and 33 show changes with elapsed time of the effective stress level, prevailing creep rate, and total fraction of life expired for representative fibers located in accordance with the scheme of Figure 29. Also plotted for each fiber considered is the total time which would elapse until rupture of that fiber if the stress pattern in the specimen were to be "frozen" at current values so that the stress level in the fiber would not change for the rest of the test. This appears to offer the best graphical picture of changing conditions with time of several considered.

Calculated points have been added to the curves to indicate the self-correcting features of the analysis used. In the calculations proposed the assumption of constant creep rate for even a short time interval during which stress changes still occur is admittedly false. Therefore, calculated stress changes during the initial time interval exceed the changes expected in the actual specimen. However, the calculated change in creep rate resulting from the stress change also

exceeds the actual drop, so that the stress change calculated for a succeeding time interval is less than the actual change. After a few intervals, the calculated results have errors in the opposite direction, but now the error in creep rate is also reversed. Use of smaller time increments would reduce the amplitude of these oscillations from the mean curve, but the effort expenditure per set of calculations would increase without appreciable change in the trends found for the several variables plotted.

For the Waspaloy specimen considered, initial concentration of effective stress for the outermost ring (Ring 9) was only 1.54, so that even a moderate variation in creep rates between different rings in the specimen cross section permitted the stress concentration to decrease without rapid use of rupture life. By the end of 17 hours the effective stress was below the nominal stress for all fibers in the entire notch cross section, and still the ring with the highest initial stress had used up only a little more than one third of its total life, and other rings a much smaller portion. At later times the calculations indicate that the central core of the specimen actually reaches an effective stress above that for fibers nearer the notch root. This is a consequence of the higher creep rate (for a given stress level) in fibers with a larger portion of total life expired. By the end of 250 hours the creep rates for all fibers were so nearly the same that further interaction between rings by the mechanism hypothesized should be small. At this stage of the calculations the highest stress and highest rate of life expenditure are found near the axis of the specimen and extrapolation of the trends established indicates failure will occur first for Ring No. 1 at an approximate elapsed time of from 500 to 700 hours. (The experimental rupture life, from Fig. 3, was found to be 520 hours.)

The calculations for Inconel X-550 present quite a different pattern of results. For the conditions under study changes in stress level were significant only in the outer ten percent of the notch cross section. The initial effective stress concentration was high, with the centroid of Ring 9 starting at 2-1/4 times the nominal stress (some 50,000 psi above it). Creep rates even at this high stress were not sufficiently high to allow much relaxation before a large portion of life was gone for the outermost fibers.

Rupture in this case occurs first in the outside fibers which cannot relax even to the nominal stress before all life has passed. Calculated time for initial failure of any ring was just over 47 hours. This agrees well with the curve of Figure 7 for notches heat treated after machining, and hypothesized to be free from residual-stress effects.

Satisfactory agreement between prediction and experiment in these two examples cannot be taken as proof that the analysis is sound. It does appear, however, that stress redistribution by creep-relaxation could be capable by itself of explaining the observed wide differences in notch behavior for different materials and test conditions.

According to the calculations, the amount of creep required for stress redistribution is moderate. The cumulative creep strain

calculated for the outside ring of the Waspaloy specimen was only about 1% during the first 90 hours, and 1.6% at the 260 hours time where calculations were terminated. If the 0.000032 in/in/hr creep rate at that time lasted for another 340 hours, the total creep at rupture would amount to only 2.7%. The Inconel X-550 calculations indicated slightly less than 1% creep by the time the outer ring failed.

Throughout this report initial stress concentrations have been calculated using classical theories of elasticity, including the tacit assumption of a "structureless" material which can be arbitrarily subdivided into infinitesimal elements. Deformation of the body, neglected by elasticity theory, also introduces significant error in calculations for high stress levels.

As the notch root radius is made smaller, deviations from the theoretical stress concentration factors are to be expected. Neuber developed a theory for pointed notches based on a material consisting of many small, but finite, particles. (See Chapters VIII and IX of Ref. 10). A "Technical" stress concentration factor was defined in which the half-width of an elementary particle replaced the root radius as a significant item of notch geometry. It was shown that this new theory is needed only in the very limited zone of strong stress variation at the very notch root. Moreover, the technical stress concentration factor depends on the particular alloy and its condition and can be accurately determined only through careful experimentation.

With present uncertainties in technical stress concentration factors, theoretical factors have been applied for all portions of all notches analyzed in the present program. Initial stress levels calculated for specimens with rather sharp notches are undoubtedly somewhat high. Further, in cases where localized plastic flow occurs near the notch during loading zero loss of strain energy is assumed in the approximations outlined in Appendix I. This makes the calculated values still higher than those actually present. For these reasons, it might be anticipated that the calculated rupture life for a notch-weakened alloy should be less than observed results for a notched specimen free from residual machining stresses. For alloys and temperatures where creep and relaxation are rapid, on the other hand, the higher degree of initial stress concentration assumed compared to the true value could result in longer calculated life than that measured experimentally. In any case, calculations for notches with small root radii should be less accurate than those for duller notches of the same material.

SECTION IV

FUTURE WORK

Work to date has indicated that in notched-bar rupture tests, rapid relaxation of high initial stresses by creep is often associated with notch strengthening; and slow relaxation with notch weakening. Mathematical analysis has successfully explained experimental results obtained for two particular examples with quite different notch behavior.

More conditions must be examined before the range of validity of the proposed correlation between notched-bar rupture life and smooth-bar properties may be judged. Further calculations are planned to cover the materials, test temperatures and heat treatments studied in this program to date. Assuming reasonable agreement with expectations for these conditions, extensions are planned in two directions:

1. A flat specimen notched at its edges may be used instead of the cylindrical notched bar used to date. This will provide a somewhat different stress pattern and will also permit some experimental measurement of creep strains. Tests on flat specimens are planned for materials now in the program, using conventional heat treatments.

2. Experimental and analytical work using other types of material than the heat-resistant turbine-blade alloys would provide a more general test of the correlation presented in the previous section of this report.

Some further studies appear necessary to clarify effects of notch preparation methods on experimental notched-bar rupture life. Other methods for preparing notches with low residual stresses will be sought.

Although creep or relaxation properties have been shown to correlate with notch behavior, possible influence of other factors has not been evaluated. Studies are now in progress with three different heats of Waspaloy seeking a comparison between various material properties and anticipated differences in notch sensitivity among the three heats.

Even if the proposed stepwise correlation should prove adequate to estimate notch behavior without introduction of other variables, it is rather lengthy to apply and requires a large amount of experimental smooth-bar data to be known. A simpler empirical relationship for notched-bar rupture life will therefore be sought in terms of initial stress concentrations and pertinent smooth-bar properties.

BIBLIOGRAPHY

1. Voorhees, H. R., and Freeman, J. W. Notch Sensitivity of Heat-Resistant Alloys at Elevated Temperatures. Part I. Preliminary Studies of the Influence of Relaxation and Metallurgical Variables. Wright Air Development Center Technical Report 54-175 (Part I). August, 1954.

2. Carlson, R. L., MacDonald, R. J., and Simmons, W. F. Investigation on Notch Sensitivity of Heat-Resistant Alloys at Elevated Temperatures. (Rupture Strength of Notched Bars at High Temperatures.) Wright Air Development Center Technical Report 54-391, October 1954.

3. Henriksen, E. K. Residual Stresses in Machined Surfaces. Transactions American Society of Mechanical Engineers, Vol. 73, pp. 69-76, January 1951.

4. Frisch, J., and Thomsen, E. G. Residual Grinding Stresses in Mild Steel. Transactions American Society of Mechanical Engineers, Vol. 73, pp. 337-346, April 1951.

5. Letner, H. R., and Snyder, H. J. Grinding and Lapping Stresses in Manganese Oil-Hardening Steel. Transactions American Society of Mechanical Engineers, Vol. 75, pp. 873-882, July 1953.

6. Colwell, L. V., Sinnott, M. J., and Tobin, J. C. The Determination of Residual Stresses in Hardened, Ground Steel. American Society of Mechanical Engineers, Paper No. 54-A-52.

7. Colwell, L. V., Private Communications, December 1954.

8. Guarnieri, G. J. and Yerkovich, L. A. The Influence of Periodic Overstressing on the Creep Properties of Several Heat Resistant Alloys. Proceedings of the American Society for Testing Materials. Vol. 52 (1952). pp. 934-950.

9. Robinson, E. L. Effect of Temperature Variation on the Long-Time Rupture Strength of Steels. Transactions of the American Society of Mechanical Engineers, Vol. 74, No. 5. July 1952. pp. 777-781

10. Neuber, H. Theory of Notch Stresses. J. W. Edwards, Ann Arbor, Michigan, 1946

11. Hill, R. The Mathematical Theory of Plasticity. Oxford University Press, London, 1950

12. Fried, M. L. and Sachs, G. Notched Bar Tension Tests on Annealed Carbon Steel Specimens of Various Sizes and Contours. A.S.T.M. Special Technical Publication No. 87, Symposium on Deformation of Metals as Related to Forming and Service, 1948, pp. 83-117.

13. Johnson, A. E. Creep Under Complex Stress Systems at Elevated Temperatures. Proceedings, of the Institution of Mechanical Engineers, Vol. 164, (1951), pp. 432-447.

14. Soderberg, C. R. Interpretation of Creep Tests on Tubes. Transactions, American Society of Mechanical Engineers, Vol. 63, (1941), pp. 737-748.

15. Johnson, A. E. and Frost, N. E. Rheology of Metals at Elevated Temperatures. Journal of the Mechanics and Physics of Solids, Vol. 1, (1952), pp. 37-52.

APPENDIX I

APPROXIMATE METHODS FOR ESTIMATING STRESS PATTERNS ABOVE THE ELASTIC LIMIT

In some of the notched specimens tested during the present program, local stresses near the notch root exceed the elastic limit during loading. Specific expressions for distribution of stresses and strains are not available for notched tensile specimens with axial symmetry, so that one must resort to approximate methods.

Fried and Sachs (Ref. 12) took hardness traverses on sections from large notched bars of carbon steel pulled to fracture at room temperature. Contour lines of constant hardness in the fractured bars were observed to correspond closely to the photo-elastic pattern showing lines of constant shear stress in flat notched specimens pulled under tension within the elastic range. From this coincidence it was concluded that "... in a notched body (under load) the lines of constant maximum shear stress are almost identical in the plastic and in the elastic state".

At conditions studied in the present program, no change in notch geometry during loading could be detected by examination at 50 diameters magnification. Any changes which do occur are at least too small to affect elastic stress concentration factors significantly. Under these circumstances, the relative distribution of deviator stress components corresponding to the elastic state will be assumed to continue during the small plastic strains of the loading period.

Stress Patterns During Loading for a Notched Bar with Initial Localized Stresses Above the Elastic Limit

When a notched specimen is stressed below the elastic limit for all fibers, nearly all the energy associated with straining is recoverable. During plastic deformations, energy is used in changing shape of the body, with unknown energy losses in the process. Neglecting any energy loss during plastic deformation, the attainable plastic strain in any fiber would appear to be that value at which the area under the actual stress-strain curve just equals the elastic strain energy which would have been expended had elastic conditions persisted throughout loading.

To illustrate application of this expedient, Figure 34 shows use of the stress-strain curve for Inconel X-550 at 1350°F to estimate the effective stress for one condition of plastic loading. A nominal stress of 40,000 psi is assumed applied to a notch with 0.005 inch root radius and 0.424 inch diameter of bar at the notch. At a radial distance

0.9936 times the bar radius at the notch (at the centroid of Ring 9 of Fig. 29), the effective stress under elastic loading is found from Figure 28 to be 3.24 times the nominal, or 129,600 psi. The elastic strain energy (area under the modulus line) for this stress, with an elastic modulus of 23,000,000 is:

$$(1/2)(129{,}600 \text{ psi}) \left(\frac{129{,}600 \text{ psi}}{23 \times 10^6 \text{ psi/in/in}} \right) = 365 \text{ in.lb./cu.in.}$$

The area under the actual tensile curve to a total strain of 0.00615 in/in equals 102.8 + 76.3 + 84.1 + 52.5 + 49.1 = 364.8 in.lb./cu. in. Therefore, the actual effective strain under plastic conditions should be just slightly above 0.00615, and the actual effective stress under these conditions about 89,700 psi.

Though approximate, this method should satisfy the needs of the present analysis and is certainly more accurate that assuming an "ideal" plastic with an elastic region followed by a plastic region of constant stress once the yield point is exceeded.

Illustration of Proposed Calculations when Some Stresses Exceed The Elastic Limit

In Section III, calculations were presented to illustrate the proposed correlation method for a simple case where all stresses were within the elastic limit. A comparable example will now be considered for the same alloy (Waspaloy at 1500°F) but with a sharper root radius (0.040-inch) and higher nominal stress (35,000 psi). Under elastic loading with this notch the ratios of the stress components and of the effective stress to the nominal value are as follows for the centroids of the four outermost rings of Fig. 29:

Ring No.	Axial Stress Ratio (S_a/p)	Tangential Stress Ratio (S_t/p)	Radial Stress Ratio (S_r/p)	Effective Stress Ratio ($\bar{S}/p$)
9	2.36	0.735	0.070	2.04
8	2.105	0.702	0.175	1.73
7	1.88	0.669	0.260	1.46
6	1.75	0.649	0.304	1.305

The outer two rings should attain effective stresses of (2.04)(35,000) = 71,450 and (1.73)(35,000) = 60,500 psi under elastic conditions, but these values would both be greater than the elastic limit of about 50,000 psi indicated by Fig. 30. By methods illustrated in Fig. 34 the actual effective stresses for these rings were estimated to be 63,500 and 57,000 psi respectively.

These approximate effective stresses are distributed in the three principal directions in the same proportions as was indicated

for elastic loading. Thus, for Ring 9:

$$S_a = (2.36/2.04)(63,500) = 73,300 \text{ psi}$$

$$S_t = (0.735/2.04)(63,500) = 22,900 \text{ psi}$$

$$S_r = (0.070/2.04)(63,500) = 2,180 \text{ psi}$$

Completion of similar calculations for other rings and conversion to deviator components yields the stress values tabulated below.

INITIAL CONDITIONS AT THE CENTROIDS OF SEVERAL RINGS IN A NOTCHED BAR OF WASPALOY LOADED TO 35,000 PSI AT 1500°F.

(NOTCH ROOT RADIUS 0.040 IN.)

Ring No.	Deviator Stress Components (psi) S'_a	$-S'_t$	$-S'_r$	$\bar{S}$	Effective Creep Rate (in/in/hr) $\dot{e}^p$	Slope of Tensile Curve H' (psi/in/in)
9	40,510	9,890	30,610	63,500	0.072	--
8	36,630	9,620	27,010	57,000	0.029	13.6×10^6
7	33,100	9,400	23,700	51,100	0.012	17.6×10^6
6	29,690	8,810	20,870	45,760	0.0054	21×10^6

It is to be noted that $\bar{S}$ exceeds the 50,000 psi elastic limit for rings 9 through 7. The outermost ring will decline steadily in stress value; i.e., behave elastically during subsequent stress redistribution. In contrast, rings (8) and (7) will rise in stress during early stages of the calculations. The slopes (H') of the tensile curve for these two rings at their effective stresses have been added to the tabulation.

Calculations similar to those in Section III will show an initial creep-rate difference of 0.041 in/in/hr in the axial direction at the interface between rings (9) and (8). For a time interval of 0.002 hour the axial stress change at this interface is found, by application of Eq. 10 and 14, to be:

$$\Delta S_{a)\,\text{Ring } 9} = (0.041 \text{ in/in/hr})(0.002 \text{ hr})\left(\frac{-21 \times 10^6 \text{ psi/in/in}}{1.32}\right)\left(\frac{13.6}{13.6 + 21}\right)$$
$$= -510 \text{ psi.}$$

$$\Delta S_{a)\text{Ring } 8} = (0.041 \text{ in/in/hr})(0.002 \text{ hr})\left(\frac{+21 \times 10^6 \text{ psi/in/in}}{1.32}\right)\left(\frac{13.6}{13.6 + 21}\right)$$
$$= +510 \text{ psi.}$$

In the second cycle of calculations, a new value of H' is found for ring (8) corresponding to the new effective stress. After a few cycles the stress level of this ring will no longer increase, but will start to decline. Then the Area-Modulus Factor reverts to the simple form $\overset{-}{+} G \left(\frac{A_n}{A_n + A_{n-1}} \right)$.

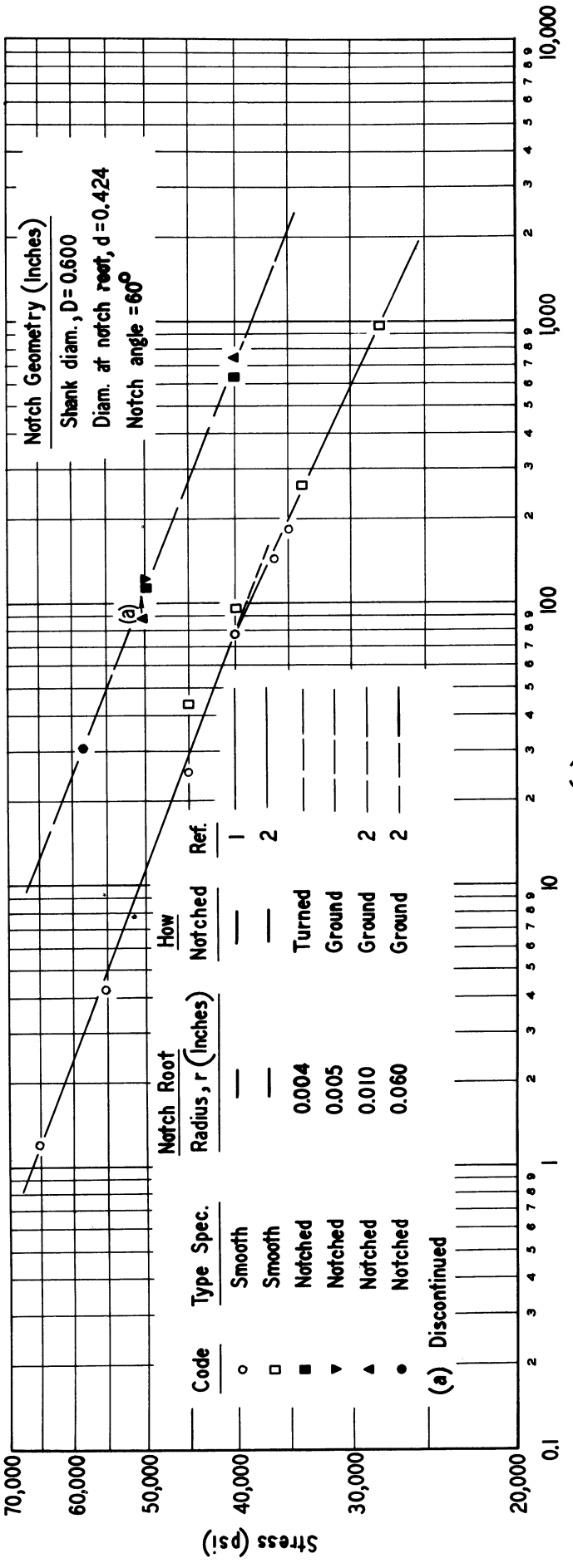

FIG. 1 - STRESS VERSUS RUPTURE LIFE AT 1350°F FOR SMOOTH AND NOTCHED BARS OF S-816 WITH CONVENTIONAL HEAT TREATMENT.

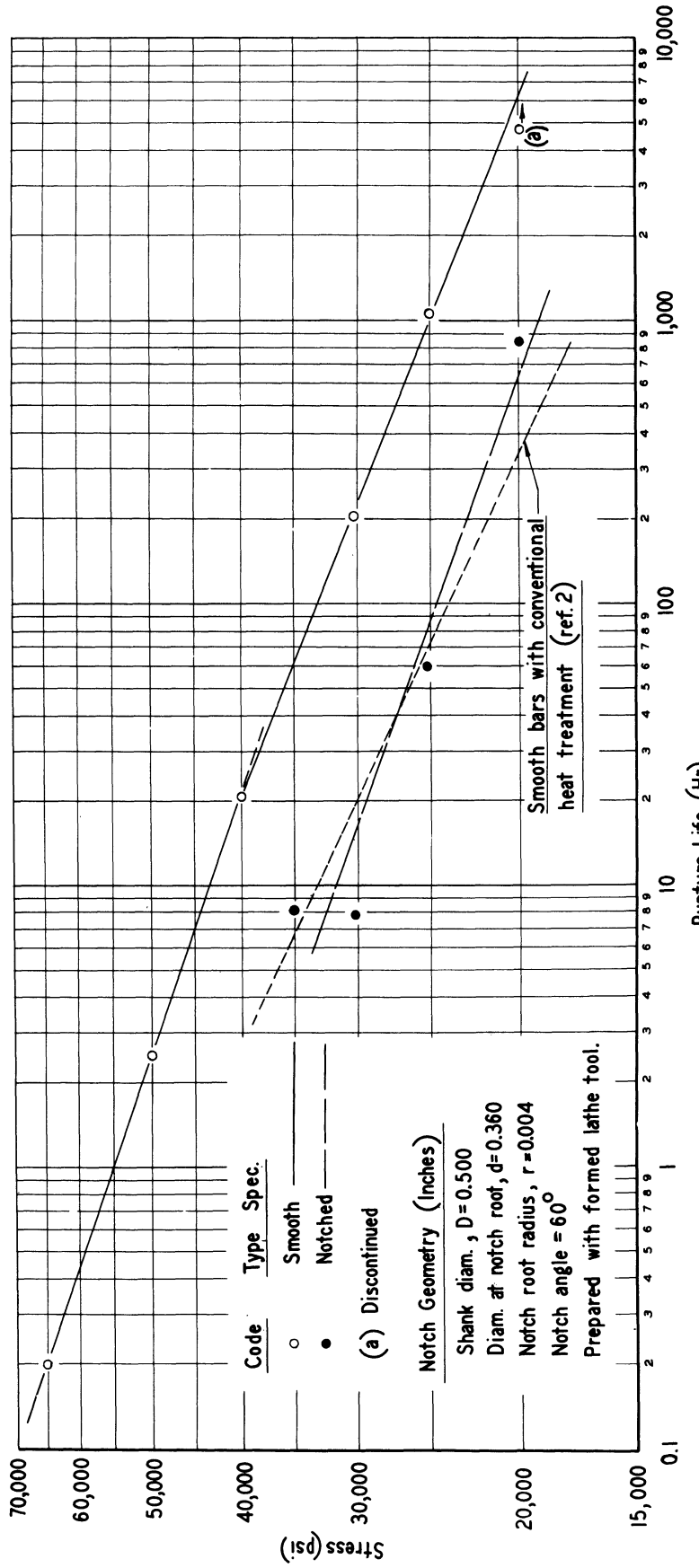

FIG. 2 – STRESS VERSUS RUPTURE LIFE AT 1500°F FOR SMOOTH AND NOTCHED BARS OF S-816 ROLLED BETWEEN SOLUTION AND AGING TREATMENTS. (2325°F, 1 HR., W.Q. + 13.5% RED. AT 1200°F + 1400°F, 12 HR., A.C.)

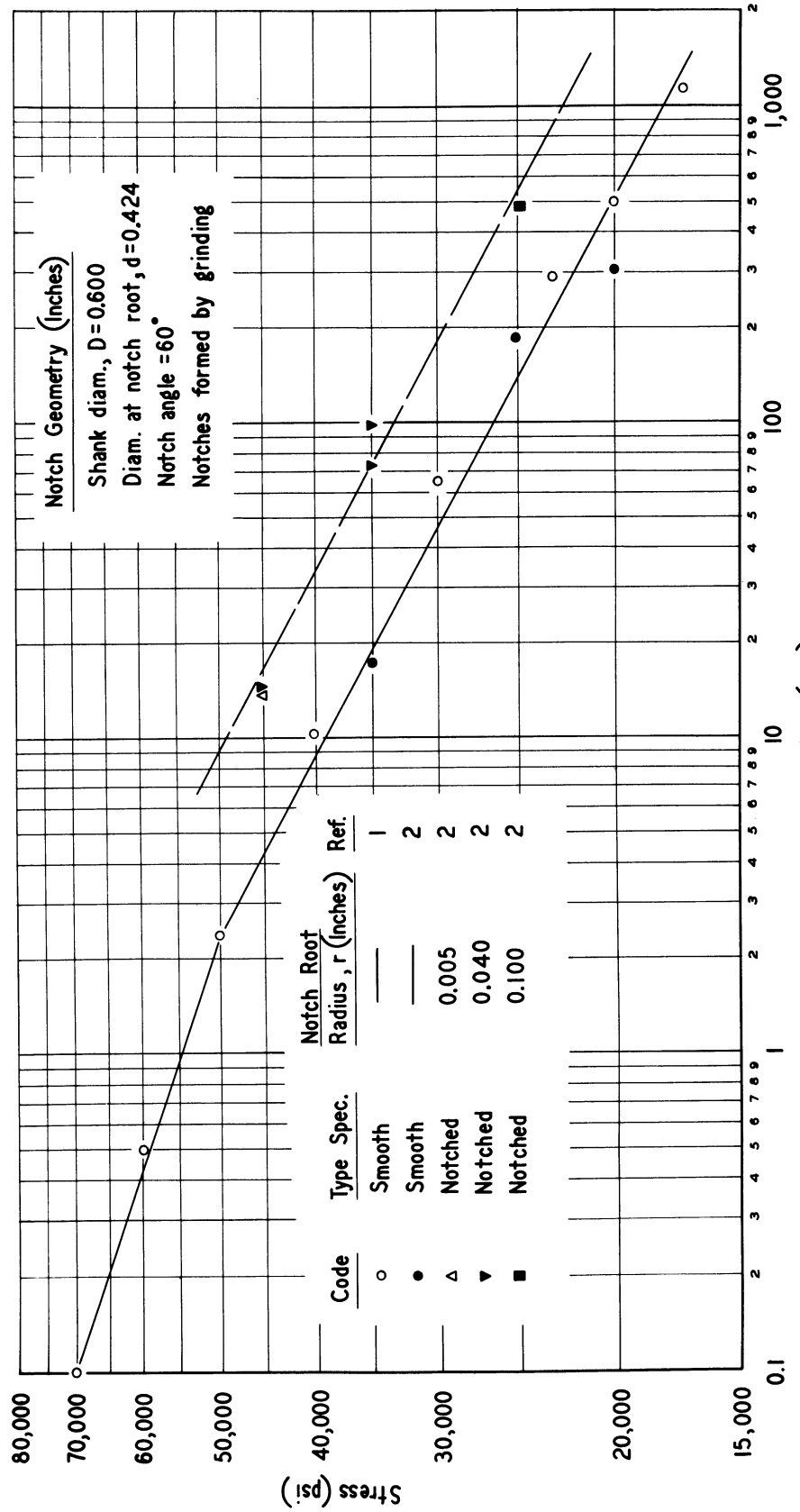

FIG. 3 — STRESS VERSUS RUPTURE LIFE AT 1500°F FOR SMOOTH AND NOTCHED BARS OF WASPALOY (HEAT 44036) WITH CONVENTIONAL HEAT TREATMENT.

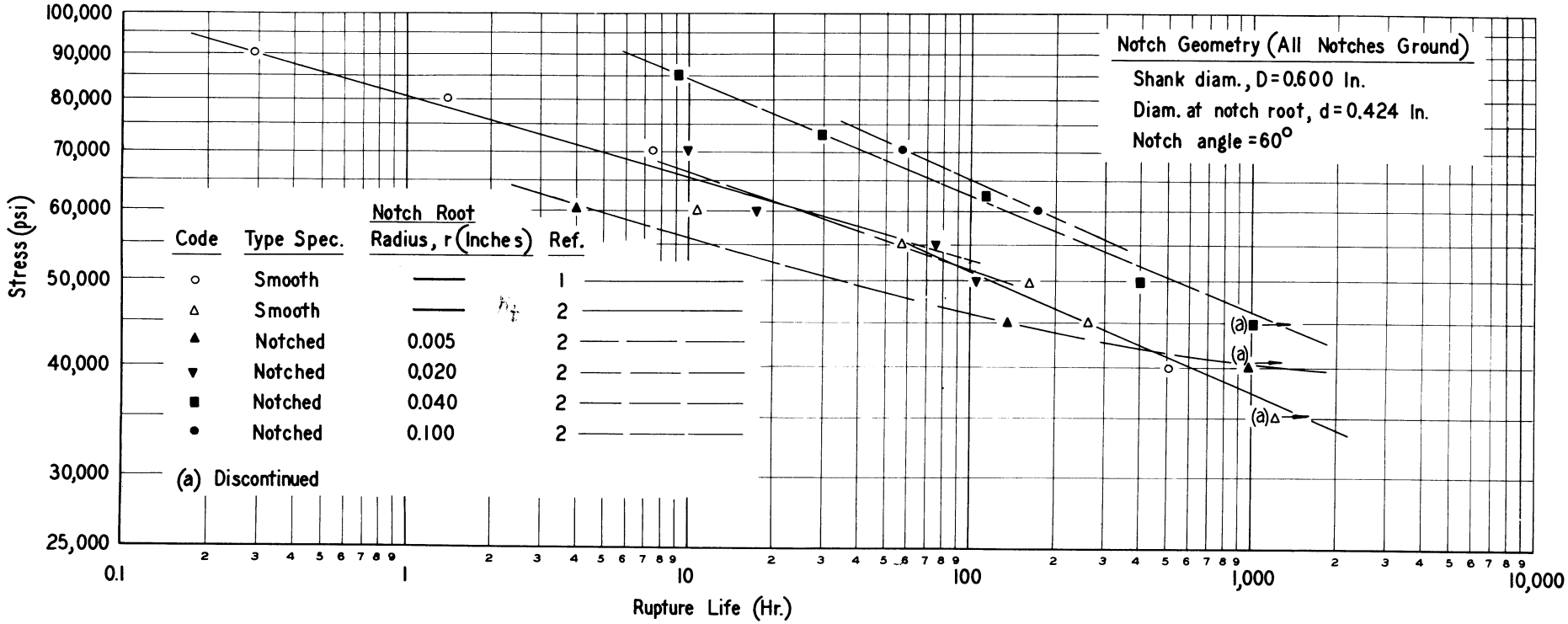

FIG. 4 – STRESS VERSUS RUPTURE LIFE AT 1350°F FOR SMOOTH AND NOTCHED BARS OF WASPALOY WITH CONVENTIONAL HEAT TREATMENT. (HEAT 44036)

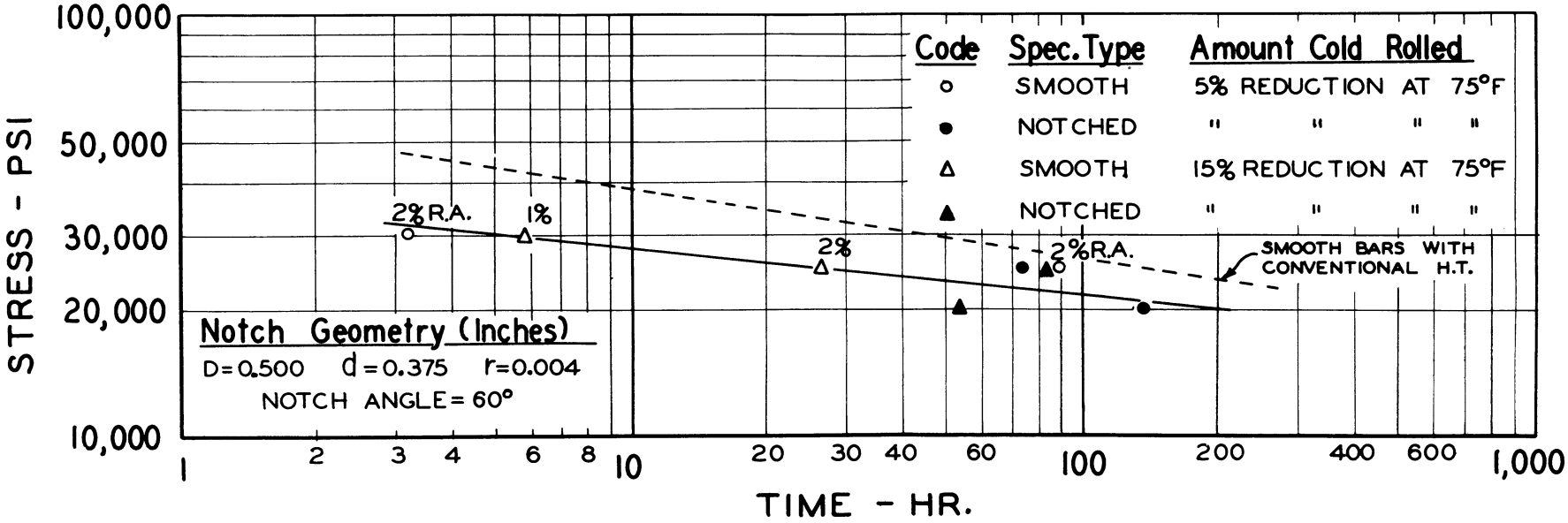

FIG. 5 - STRESS VERSUS RUPTURE TIME AT 1500°F FOR SMOOTH AND NOTCHED BARS OF WASPALOY COLD ROLLED BETWEEN CONVENTIONAL SOLUTION AND AGING TREATMENTS. (ALL NOTCHES TURNED.)

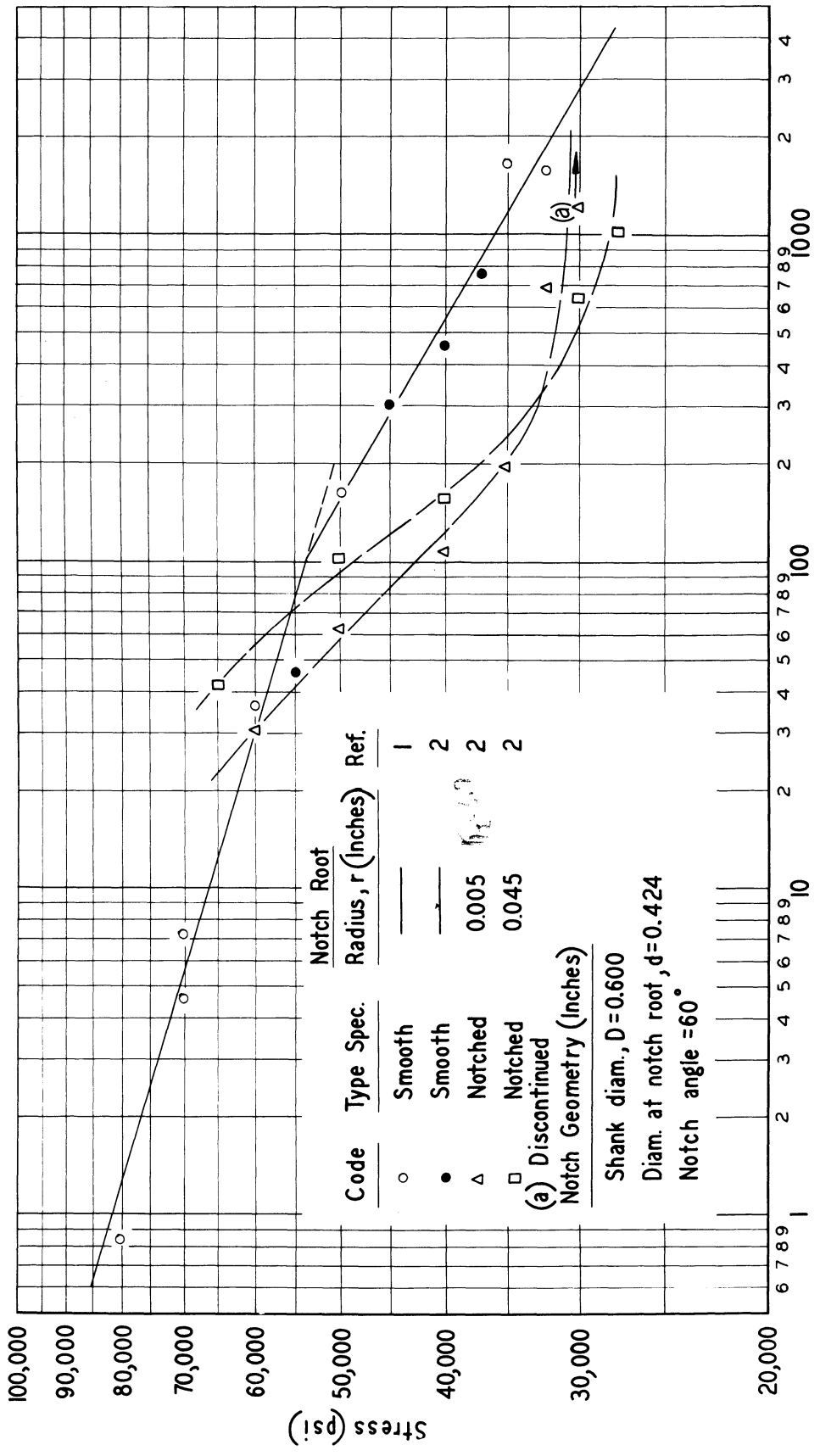

FIG. 6 — STRESS VERSUS RUPTURE LIFE AT 1350°F FOR SMOOTH AND NOTCHED BARS OF INCONEL X-550 WITH CONVENTIONAL HEAT TREATMENT. (NOTCHES FORMED BY GRINDING)

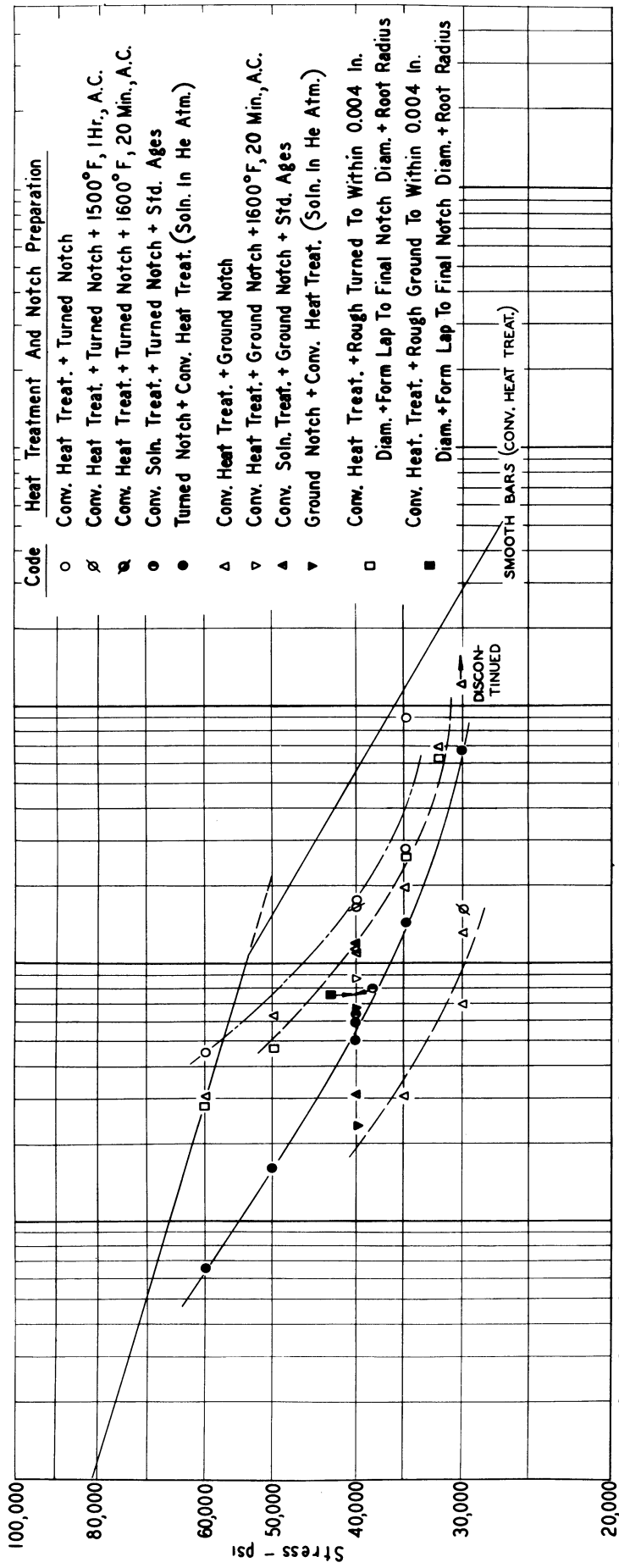

FIG. 7 — EFFECT OF METHOD OF NOTCH PREPARATION ON NOTCHED-BAR RUPTURE LIFE OF INCONEL X-550 AT 1350°F.

Notch Geometry
D = 0.600 inch
d = 0.424 inch
r = 0.005 inch

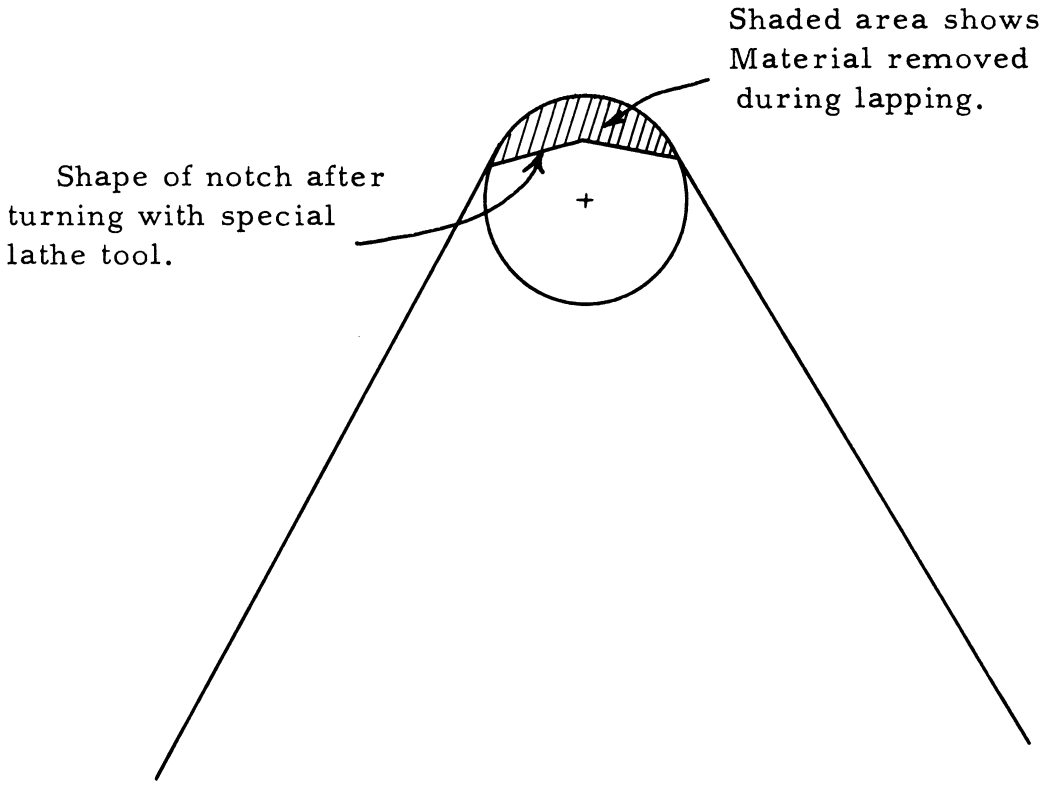

FIG. 8 - SKETCH ILLUSTRATING NOTCH PREPARATION BY FORM LAPPING.

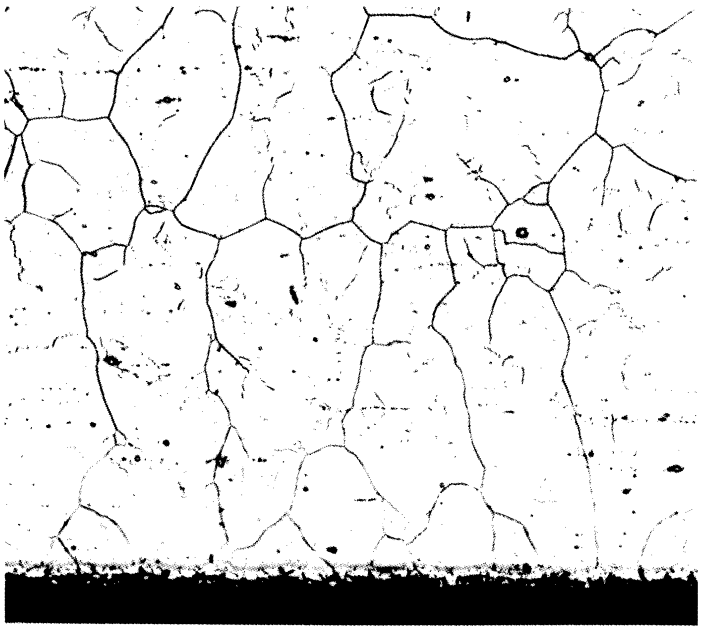

X 100 D 55-182

(a.) Columnar Grains Near Notch Turned Before Conventional Heat Treatment.

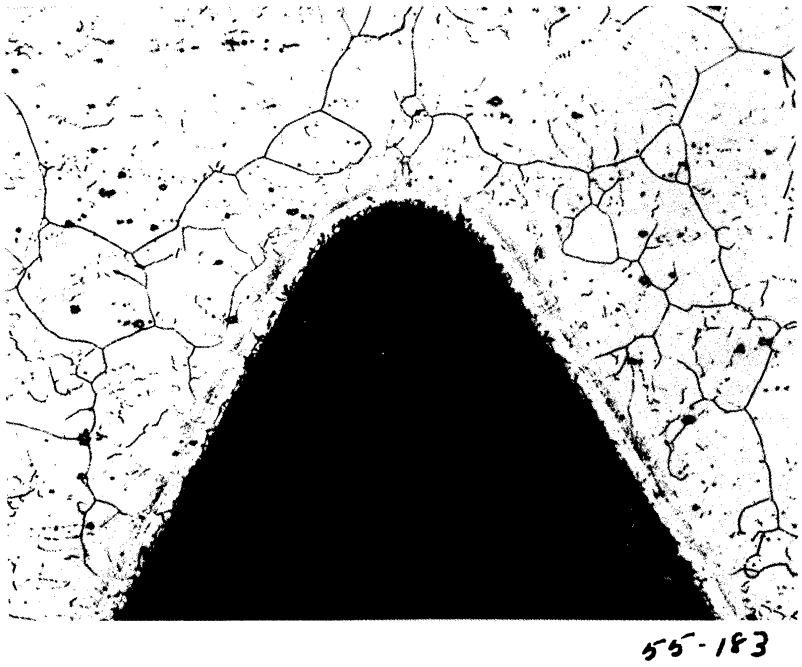

55-183

(b.) Structure Near Notch Ground Before Heat Treatment.

Figure 9. Photomicrographs Illustrating Metallographic Features in Specimens of Inconel X-550 Heat Treated after Notch Preparation.

Figure 9. (continued)

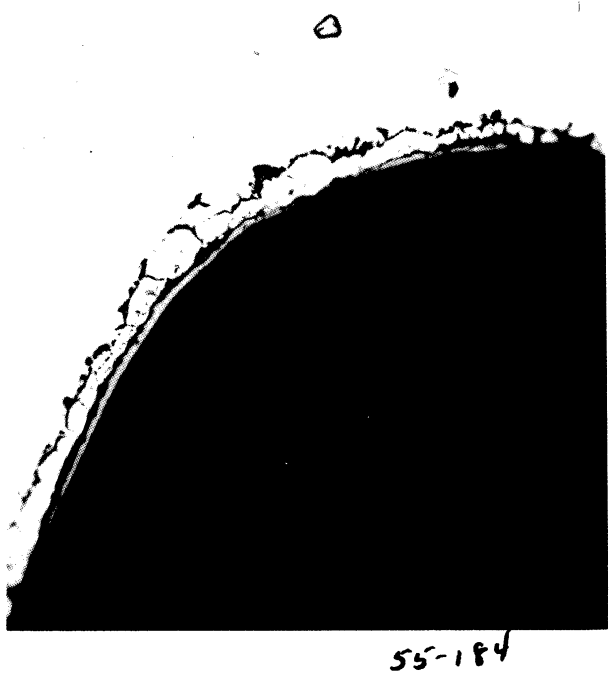

X 500 D

(c.) Surface Alteration from Heat Treatment Used. (Not etched)

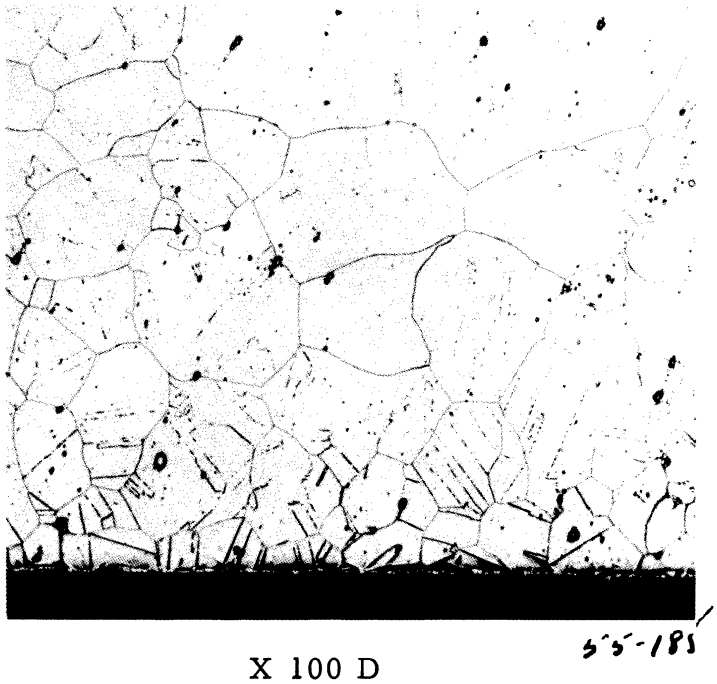

X 100 D

(d.) Twins Near Notch Turned between Solution and Aging Steps.

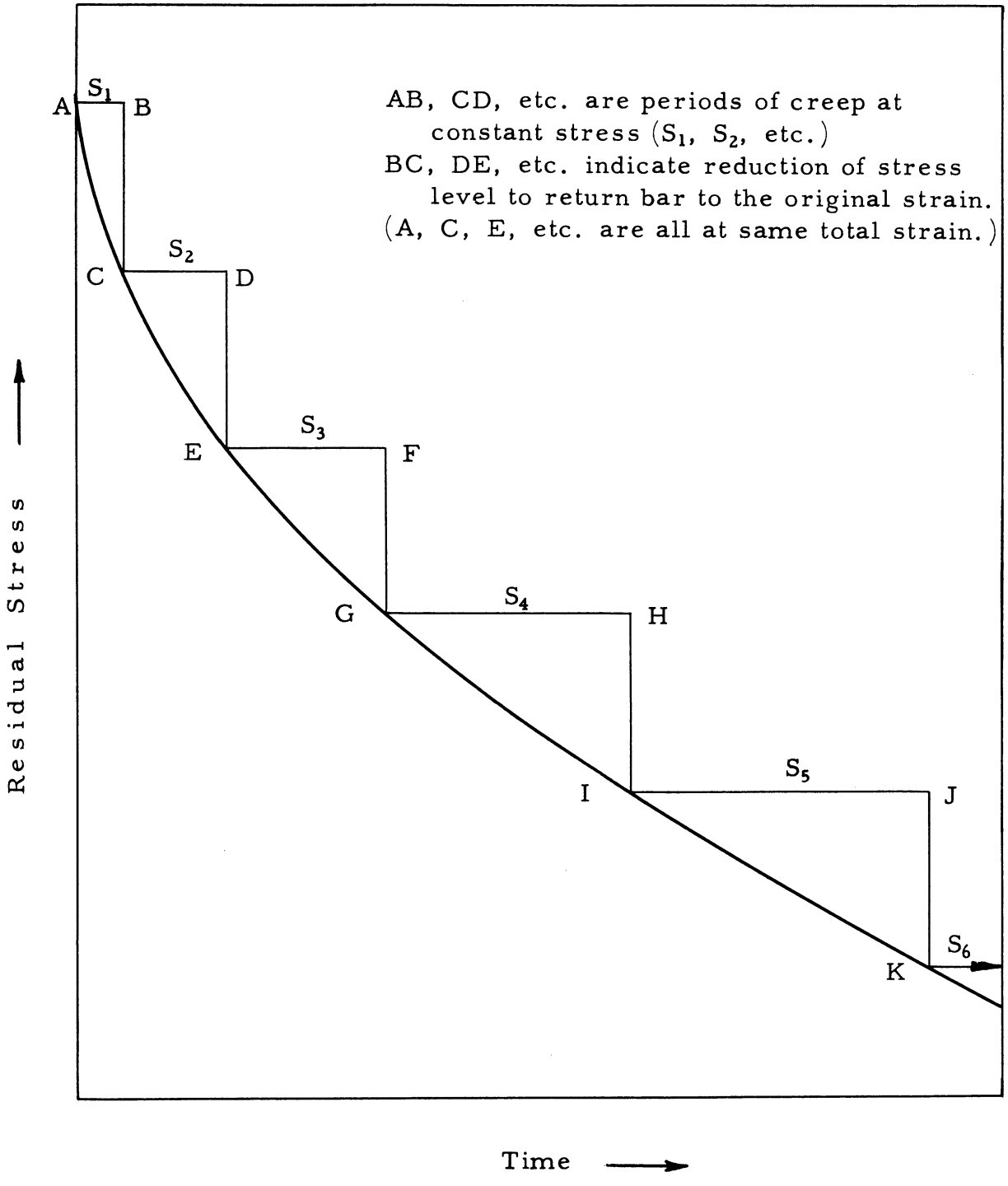

FIG. 10 - STEP-WISE RELAXATION TEST OF A SMOOTH SPECIMEN IN PURE TENSION.

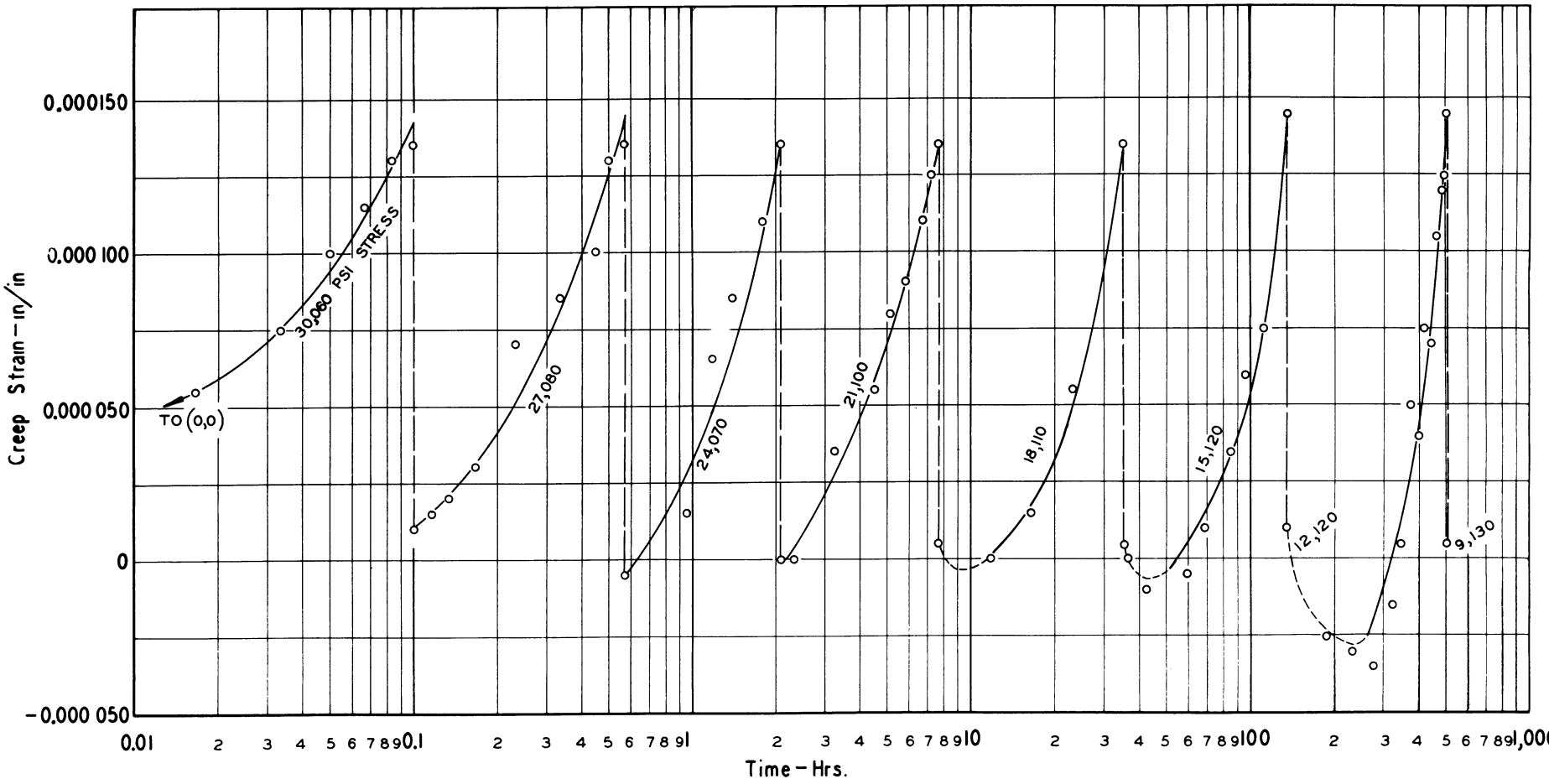

FIG. 11 - EXPERIMENTAL RELAXATION DATA FOR A WASPALOY SPECIMEN AT 1500°F WITH 30,060 PSI INITIAL STRESS.

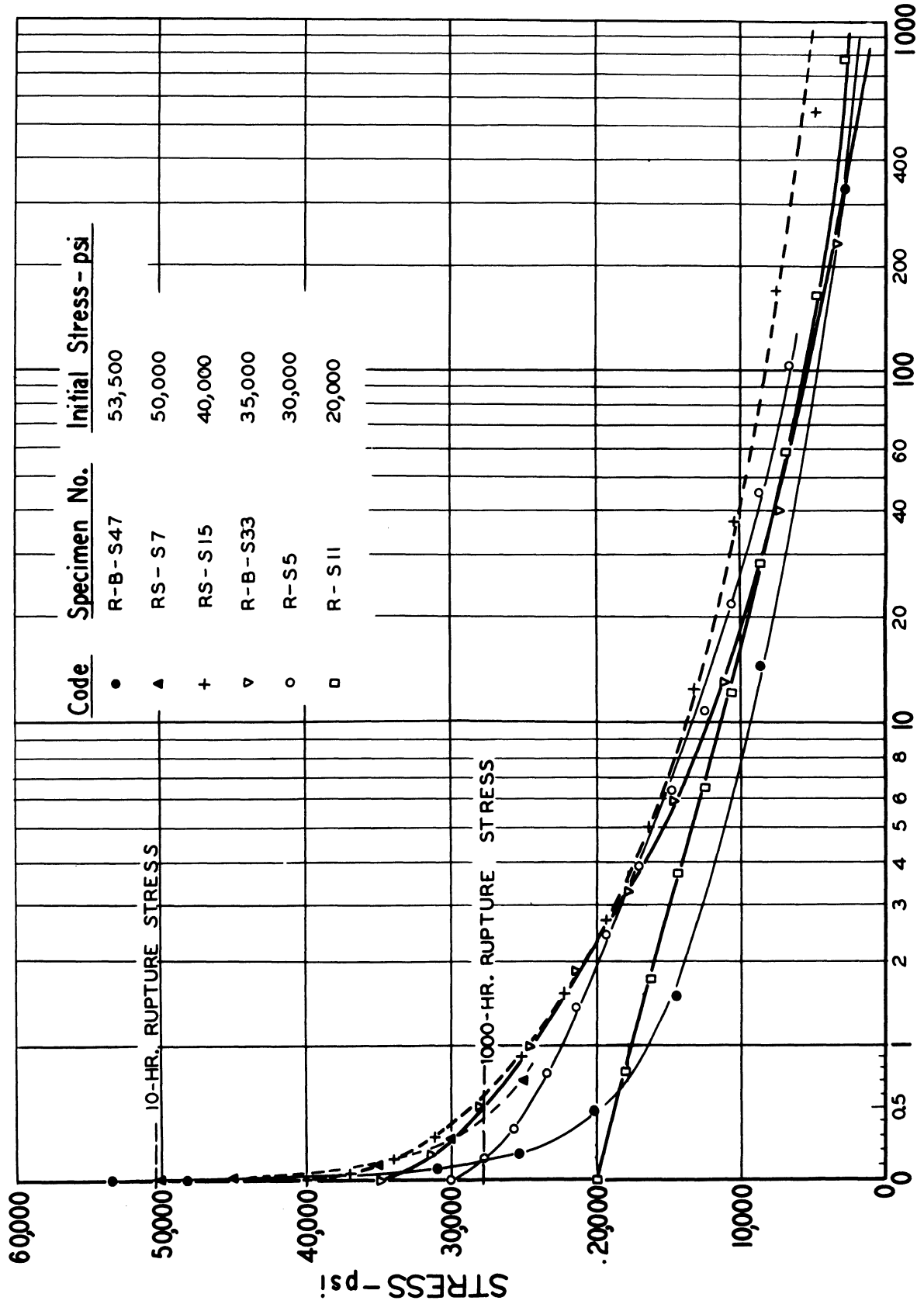

FIG. 12 - RELAXATION CHARACTERISTICS AT 1350°F FOR S-816 WITH CONVENTIONAL HEAT TREATMENT.

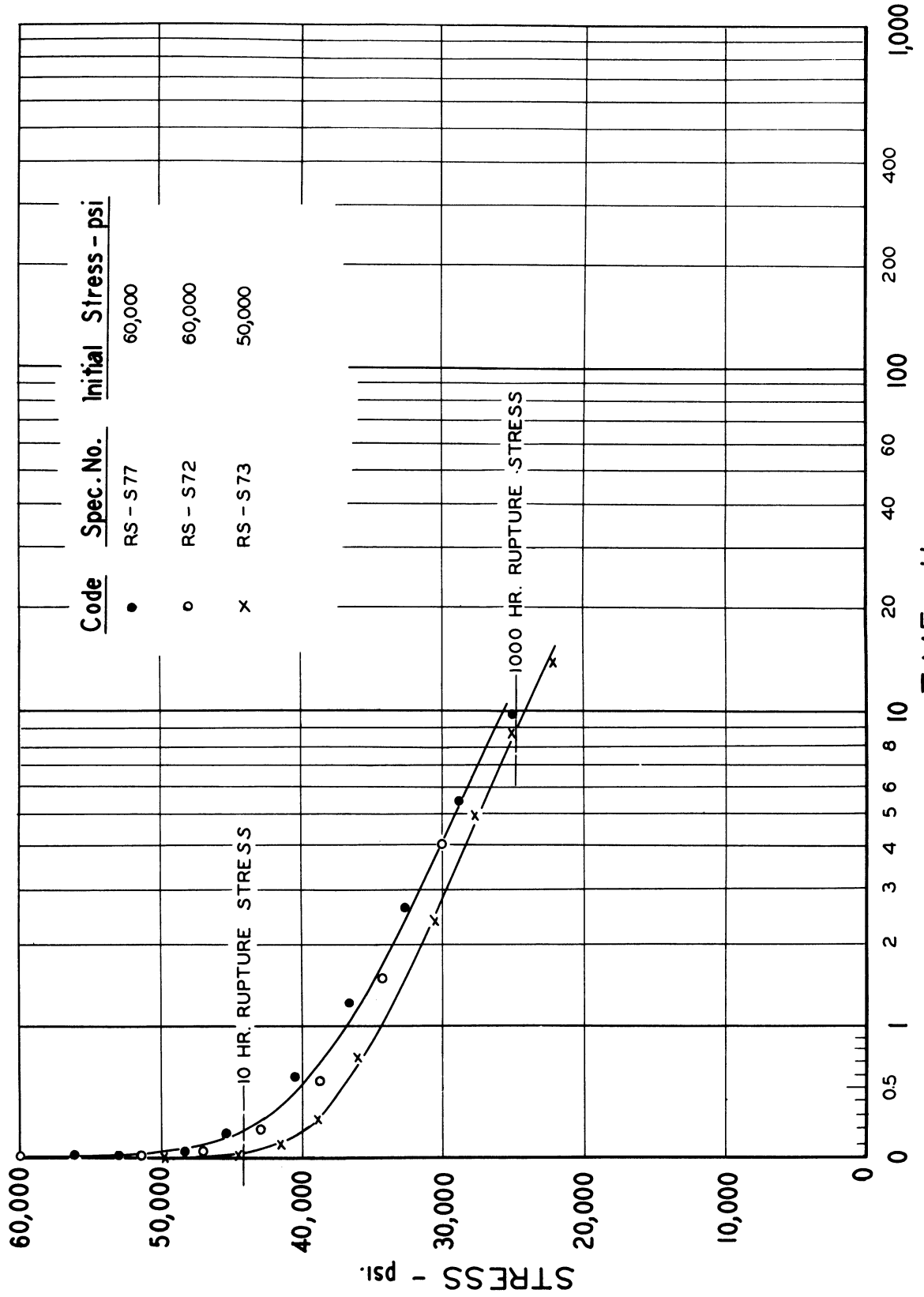

FIG. 13 - RELAXATION CHARACTERISTICS AT 1500°F OF S-816 ROLLED AFTER SOLUTION TREATMENT. (2325°F, 1 HR, W.Q. + 13.5% RED. AT 1200°F + 1400°F, 12 HR, A.C.)

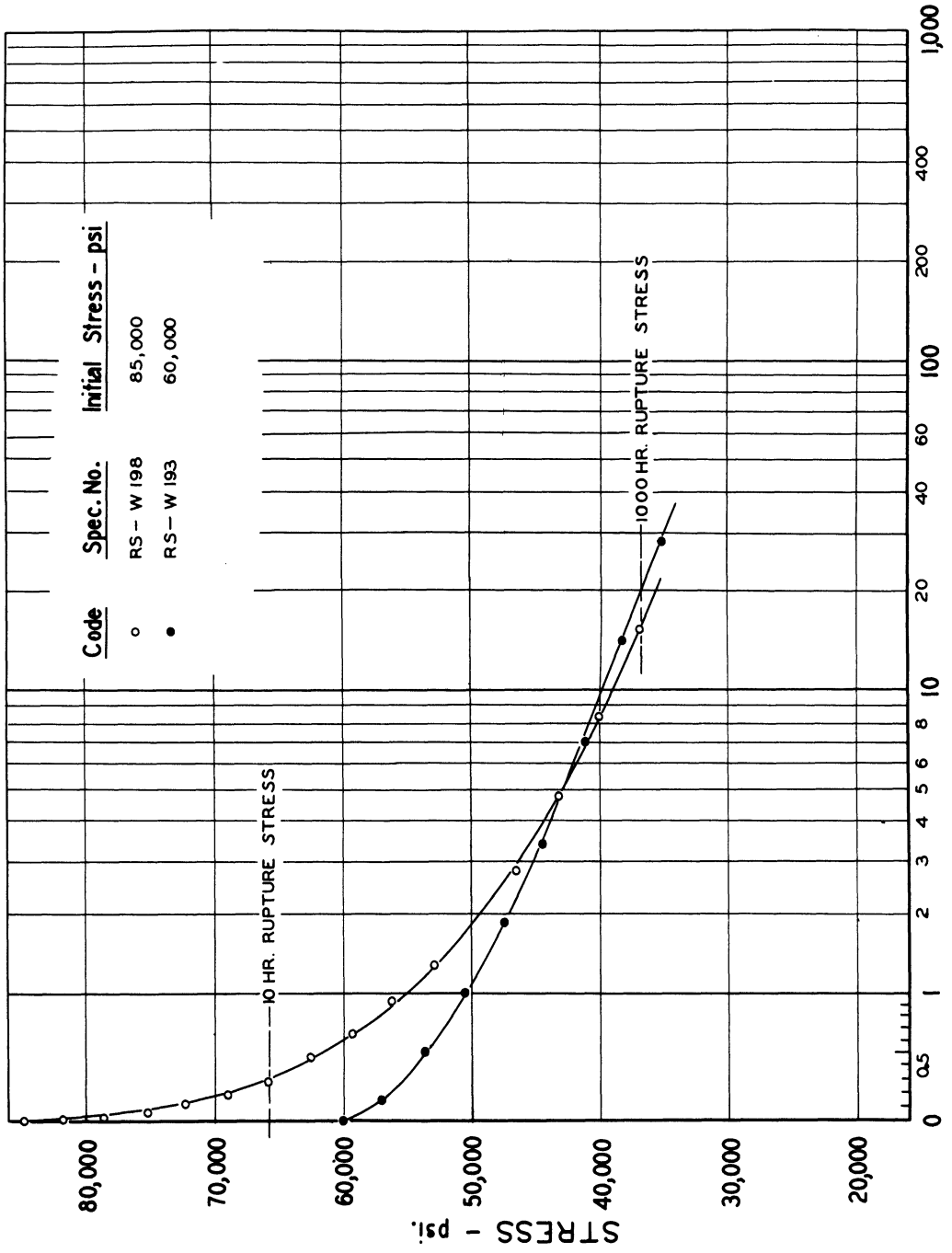

FIG. 14 - RELAXATION CHARACTERISTICS AT 1350°F OF WASPALOY WITH CONVENTIONAL HEAT TREATMENT. (1975°F, 4 HRS, A.C. + 1550°F, 4 HRS, A.C. + 1400°F, 16 HRS, A.C.)

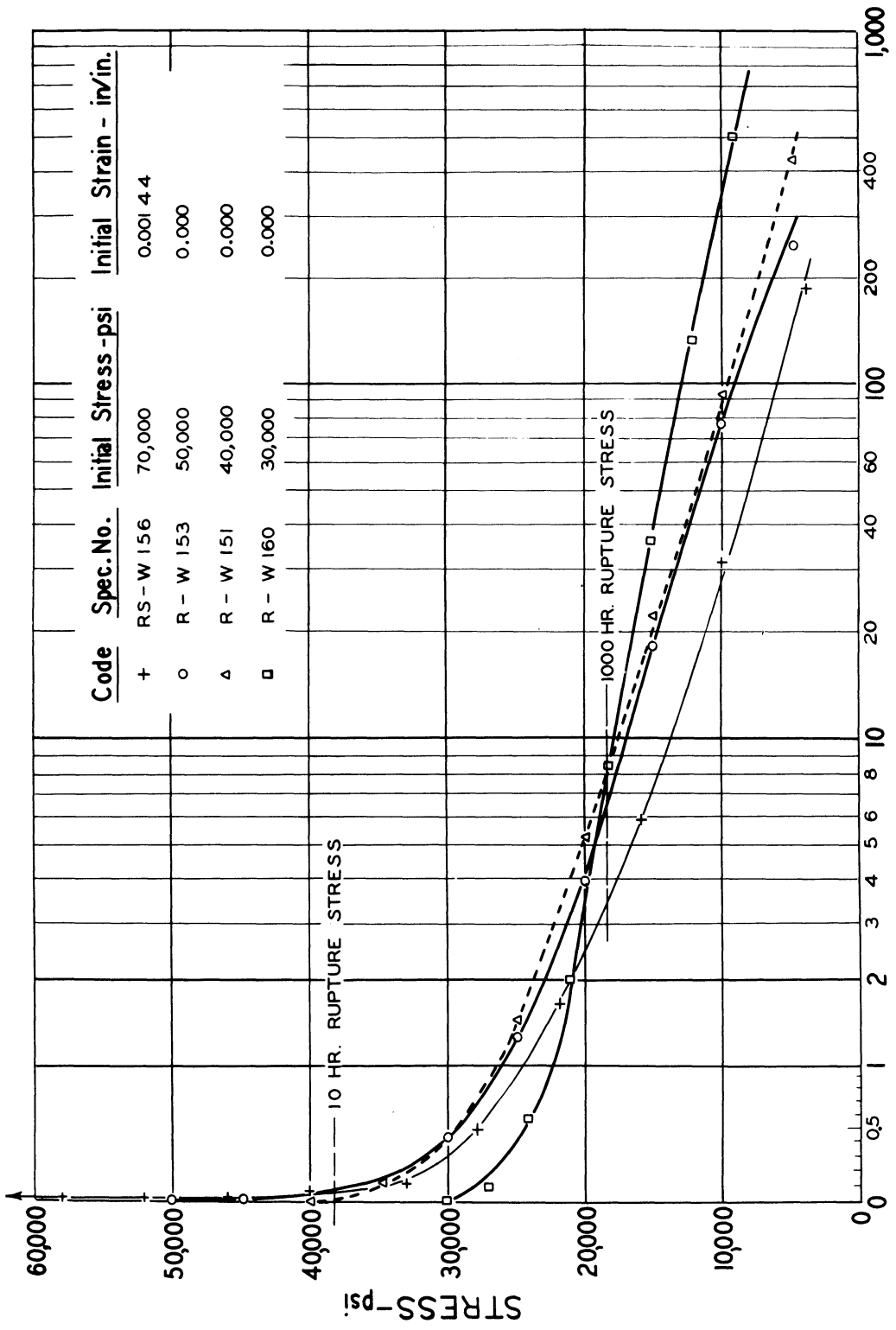

FIG.15 – RELAXATION CHARACTERISTICS AT 1500°F OF WASPALOY WITH CONVENTIONAL HEAT TREATMENT.

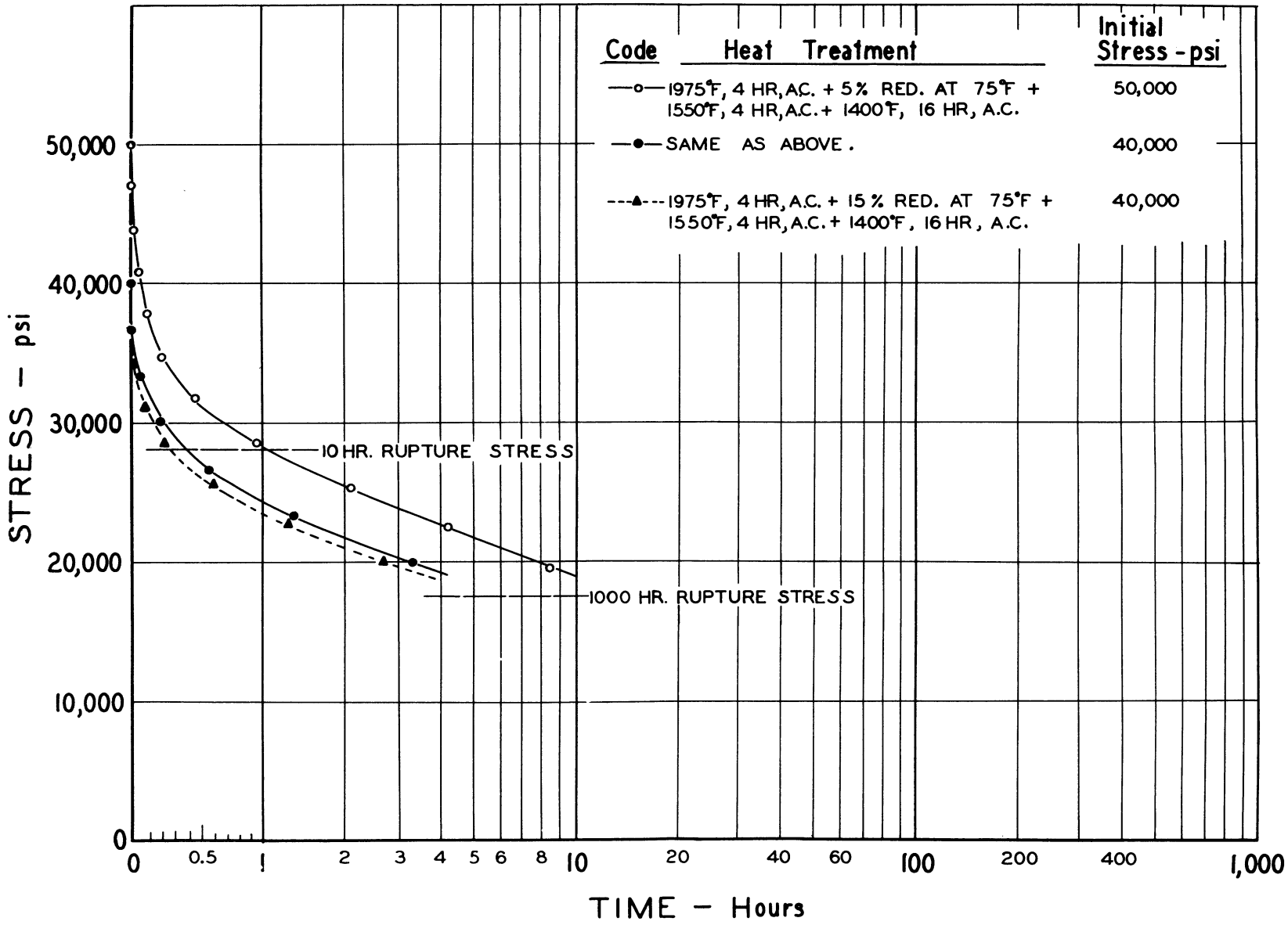

FIG. 16 - RELAXATION CHARACTERISTICS AT 1500°F OF WASPALOY COLD ROLLED BETWEEN CONVENTIONAL SOLUTION AND AGING TREATMENTS.

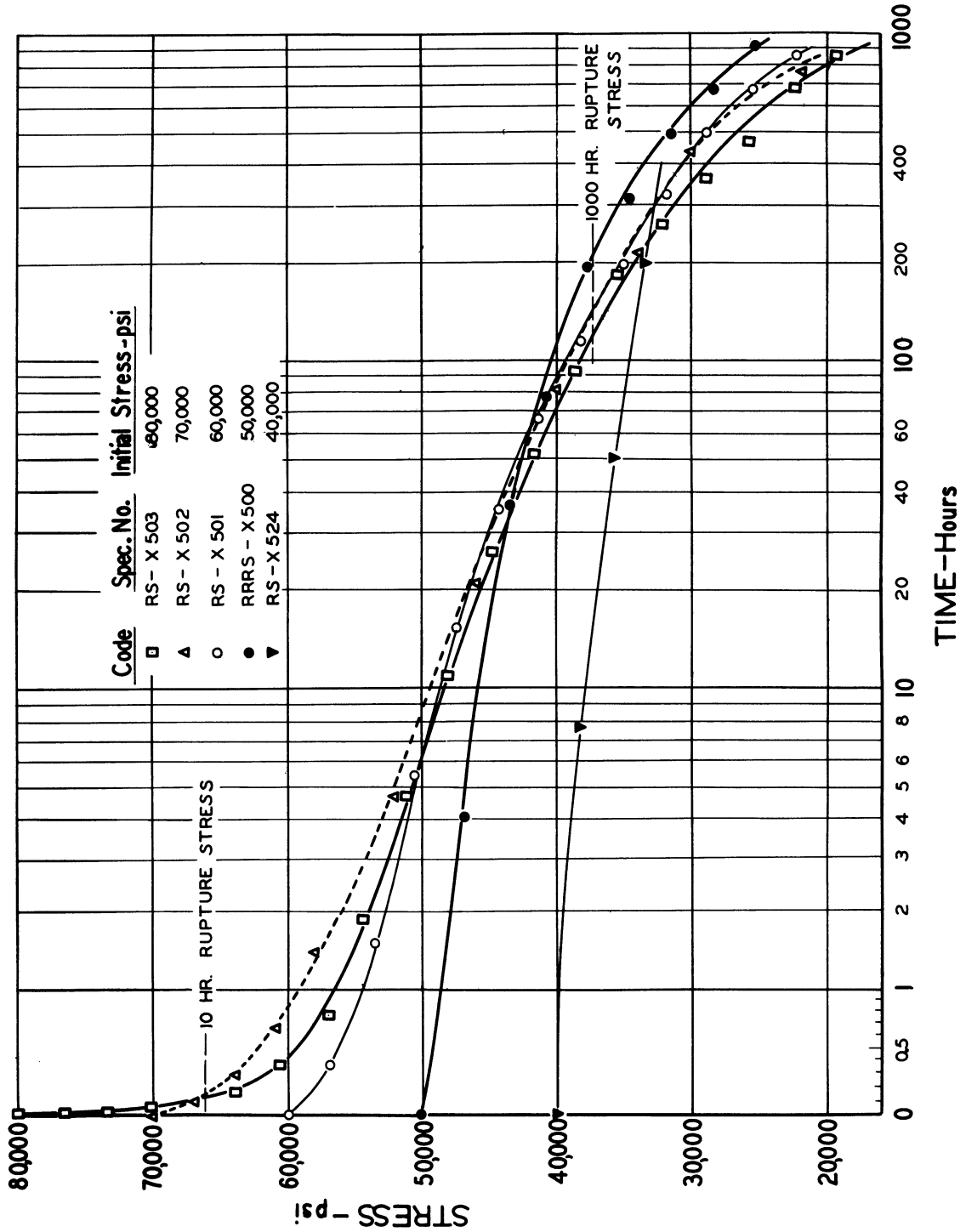

FIG.17 – RELAXATION CHARACTERISTICS AT 1350°F FOR INCONEL X-550 WITH CONVENTIONAL HEAT TREATMENT.

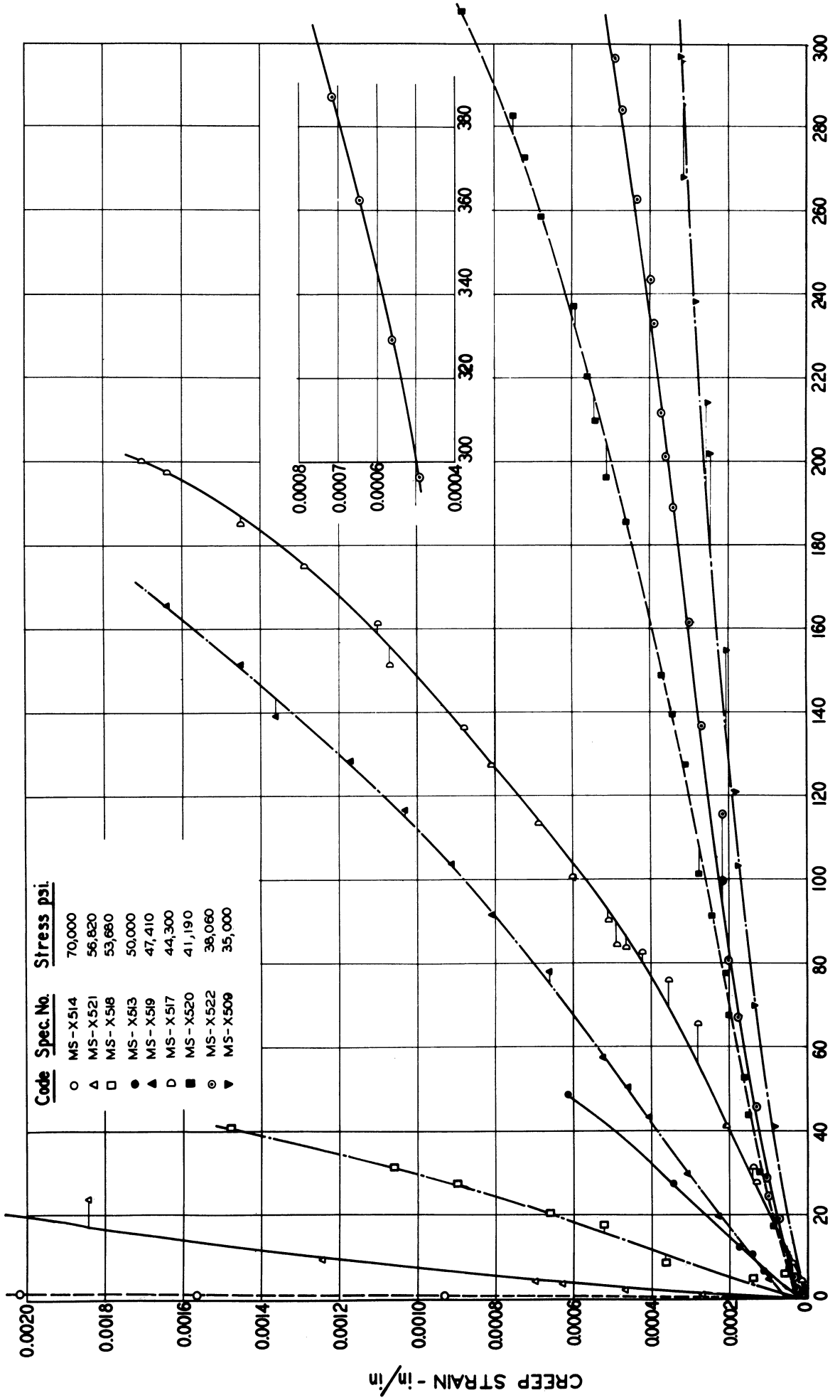

FIG. 18 - EARLY STAGES OF CREEP CURVES FOR INCONEL X-550 AT 1350° F

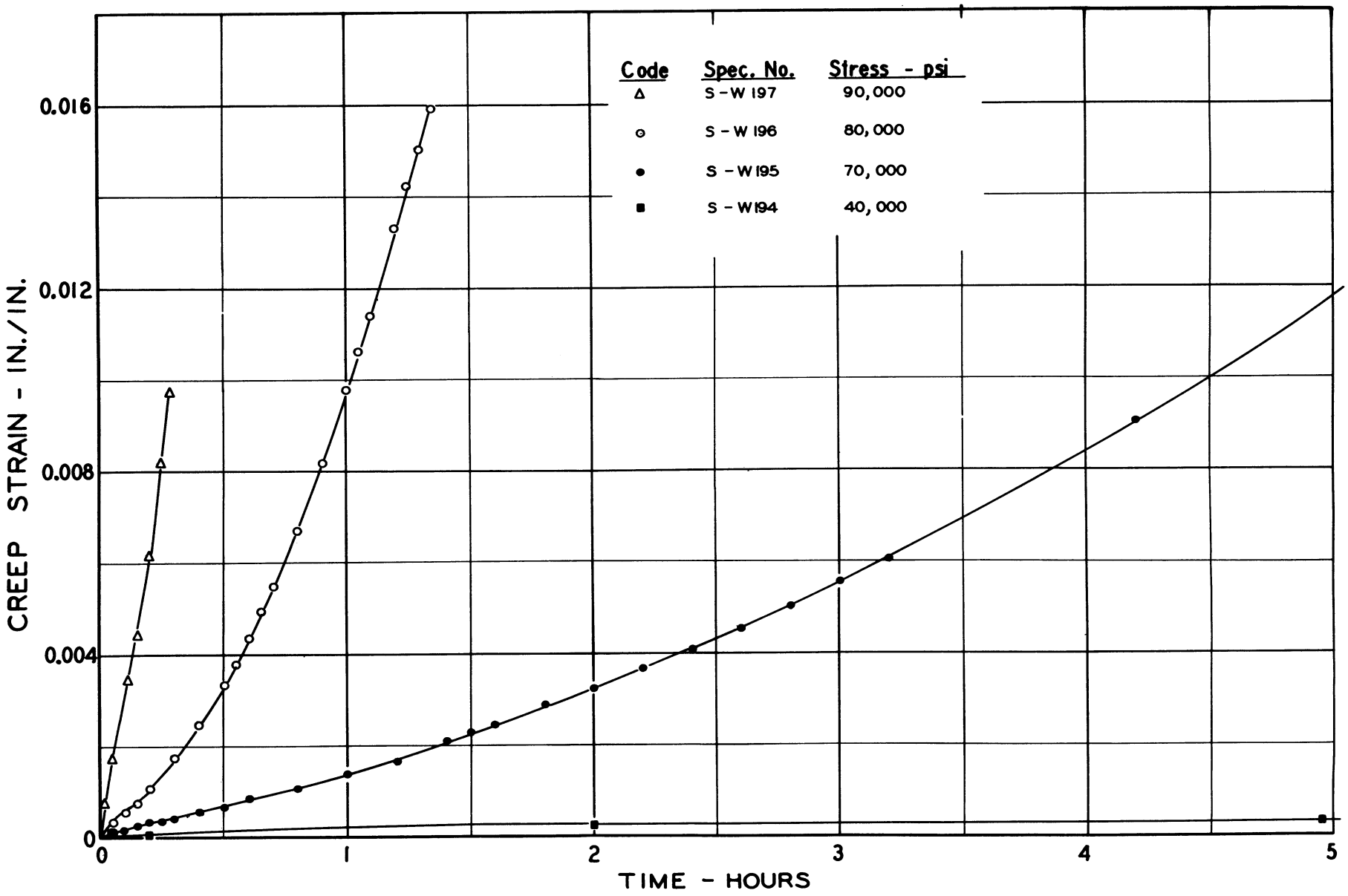

FIG. 19 - CREEP CHARACTERISTICS AT 1350°F FOR WASPALOY WITH CONVENTIONAL HEAT TREATMENT. (1975°F, 4HR, A.C. + 1550°F, 4 HR, A.C. + 1400°F, 16 HR, A.C.)

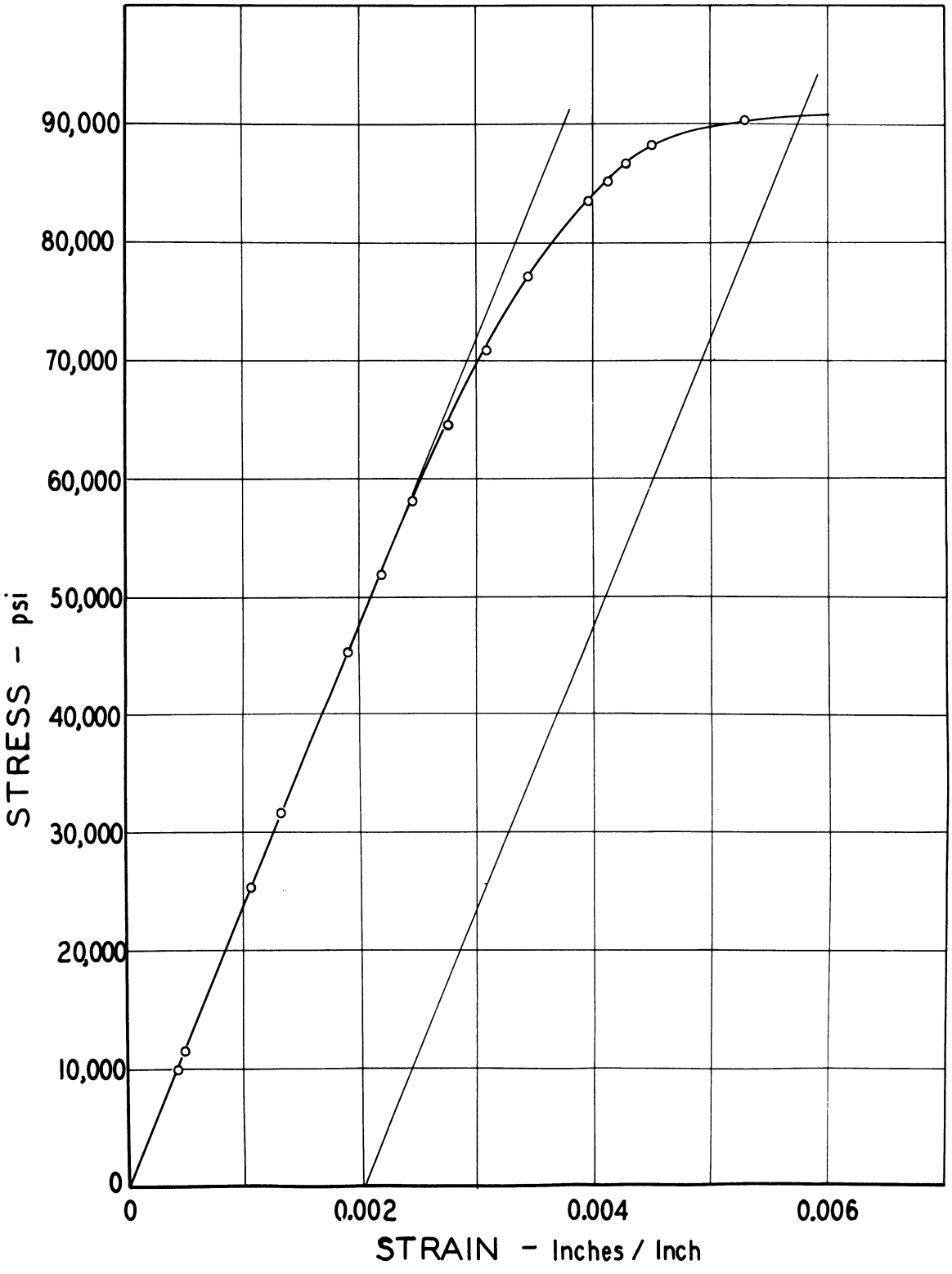

FIG. 20 - SHORT-TIME TENSILE CHARACTERISTICS AT 1350°F OF WASPALOY WITH CONVENTIONAL HEAT TREATMENT. (1975°F, 4 HR, A.C. + 1550°F, 4 HR, A.C. + 1400°F, 16 HR, A.C.)

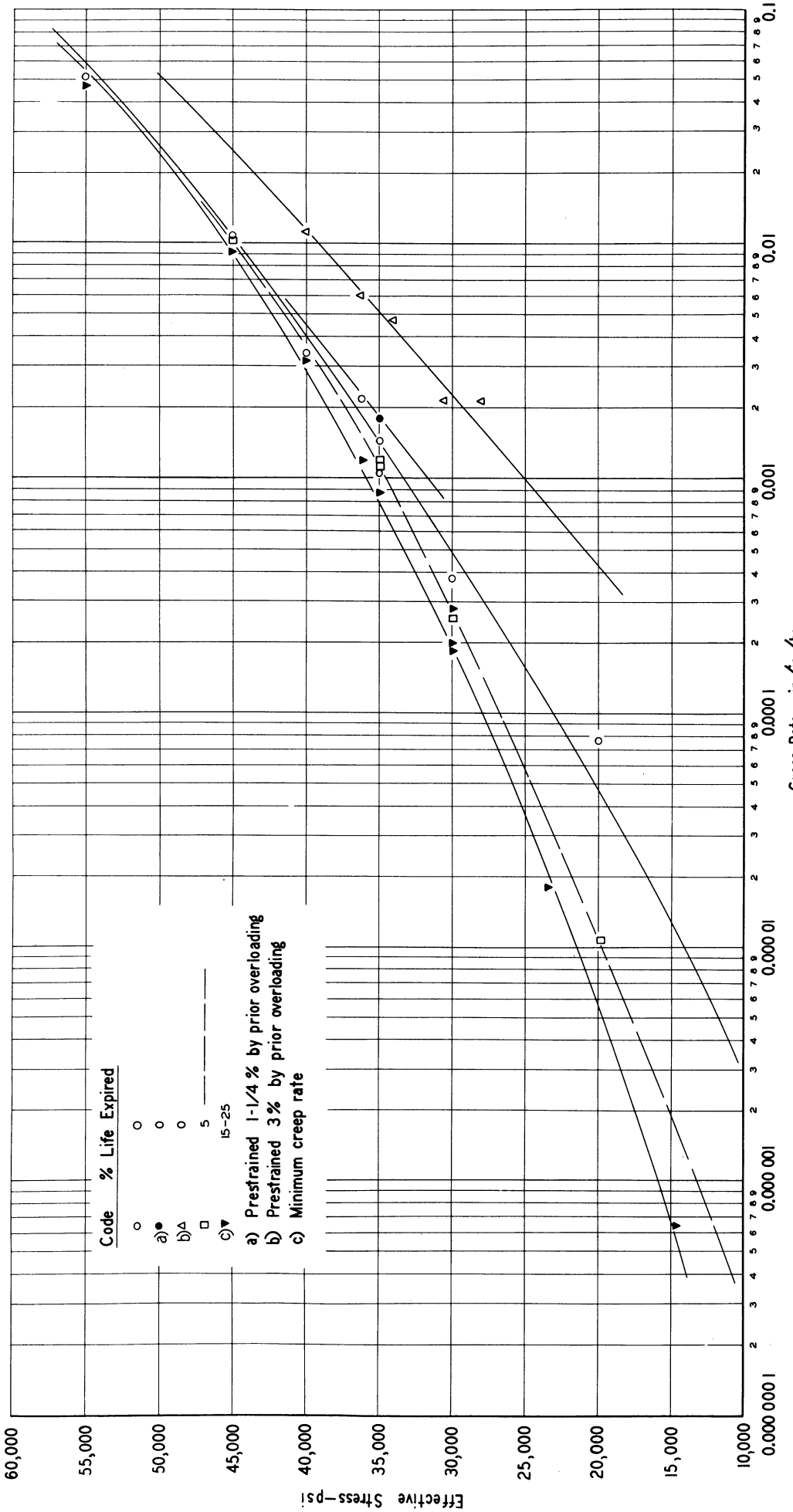

FIG. 21 – STRESS VERSUS CREEP RATE AT 1350°F FOR S-816 WITH CONVENTIONAL HEAT TREATMENT. (DECREASING RATE PERIOD)

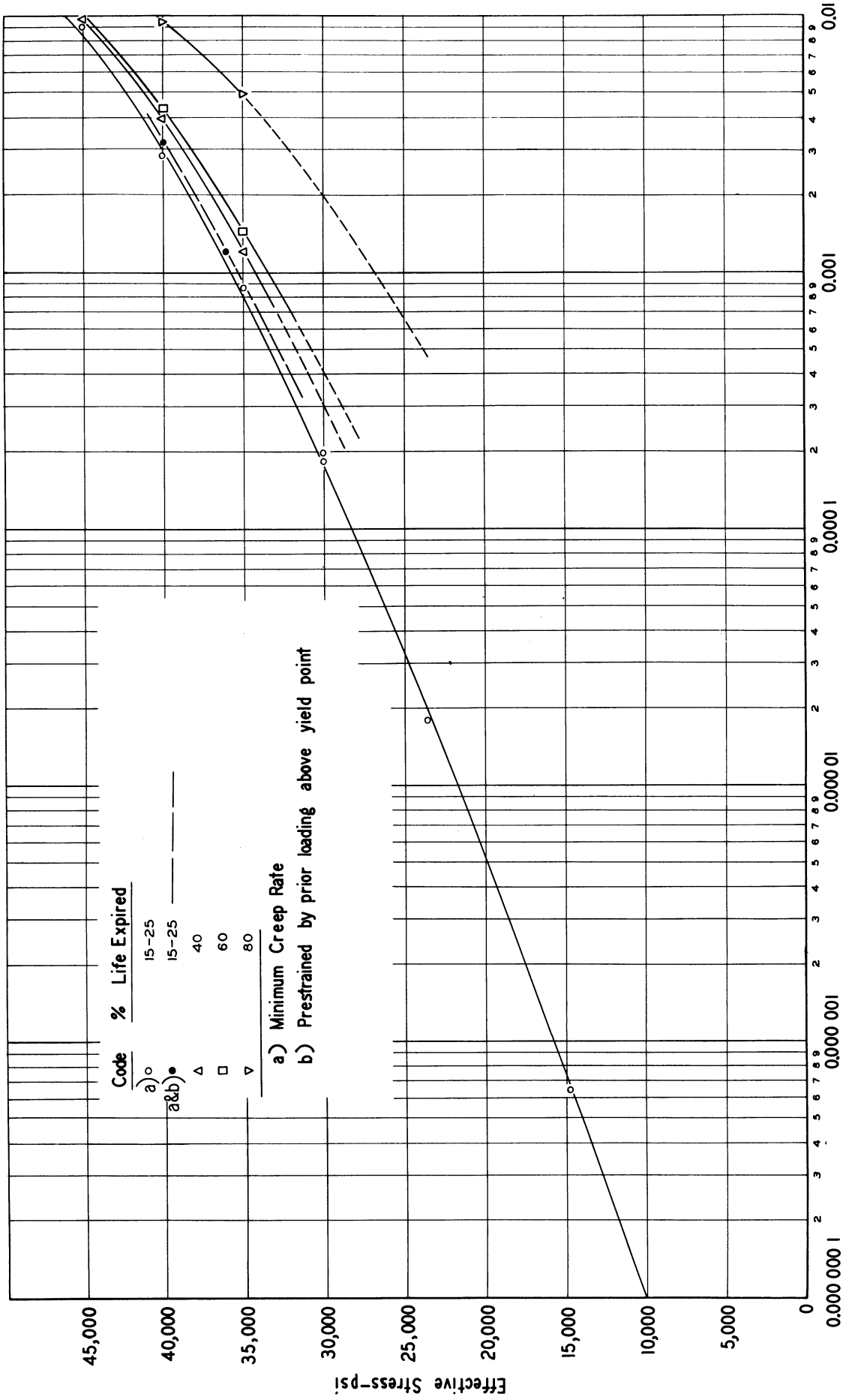

FIG. 22 - STRESS VERSUS CREEP RATE AT 1350°F FOR S-816 WITH CONVENTIONAL HEAT TREATMENT (INCREASING RATE PERIOD).

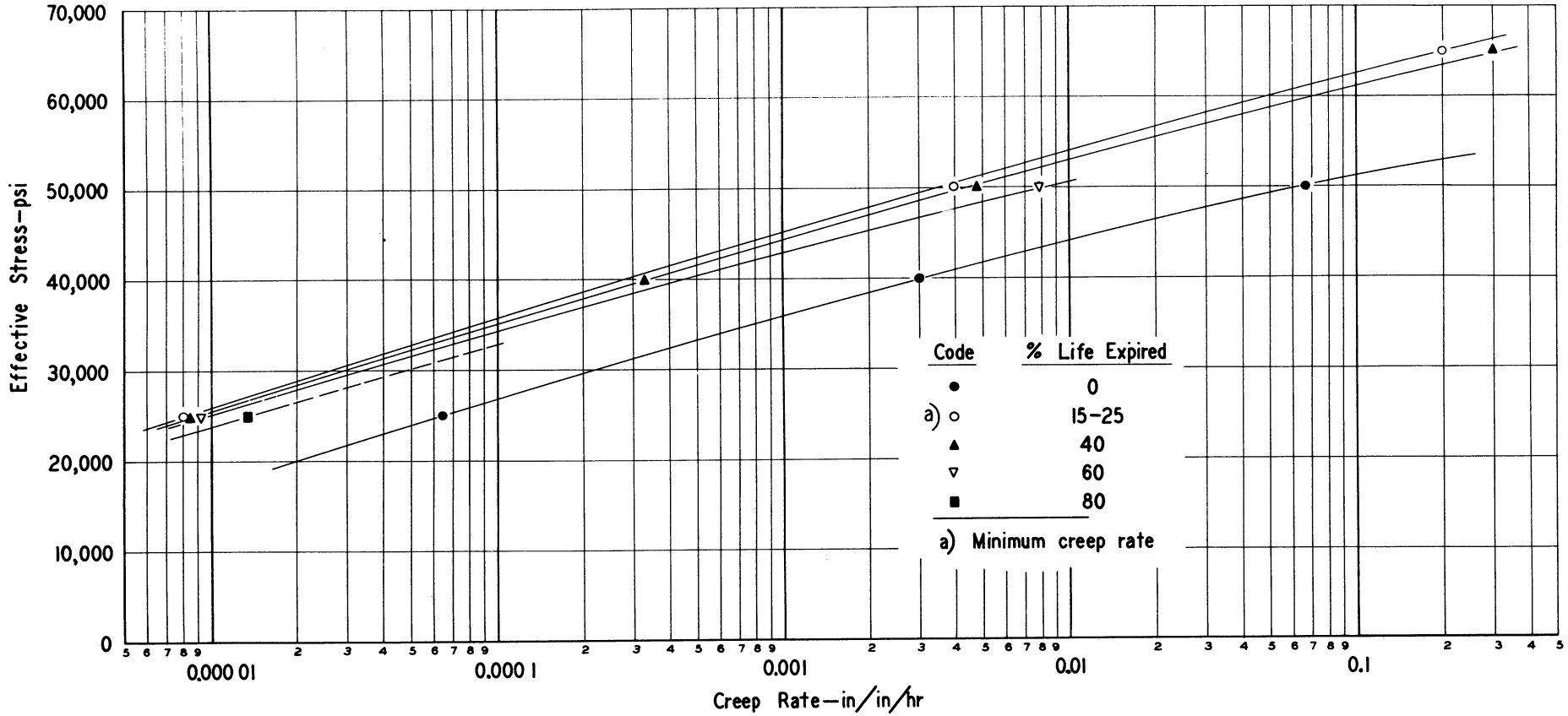

FIG. 23 — STRESS VERSUS CREEP RATE AT 1500°F FOR S-816 ROLLED BETWEEN SOLUTION AND AGING TREATMENTS. (2325°F, 1 HR., W.Q. + 13.5 % RED. AT 1200°F + 1400°F, 12 HR., A.C.)

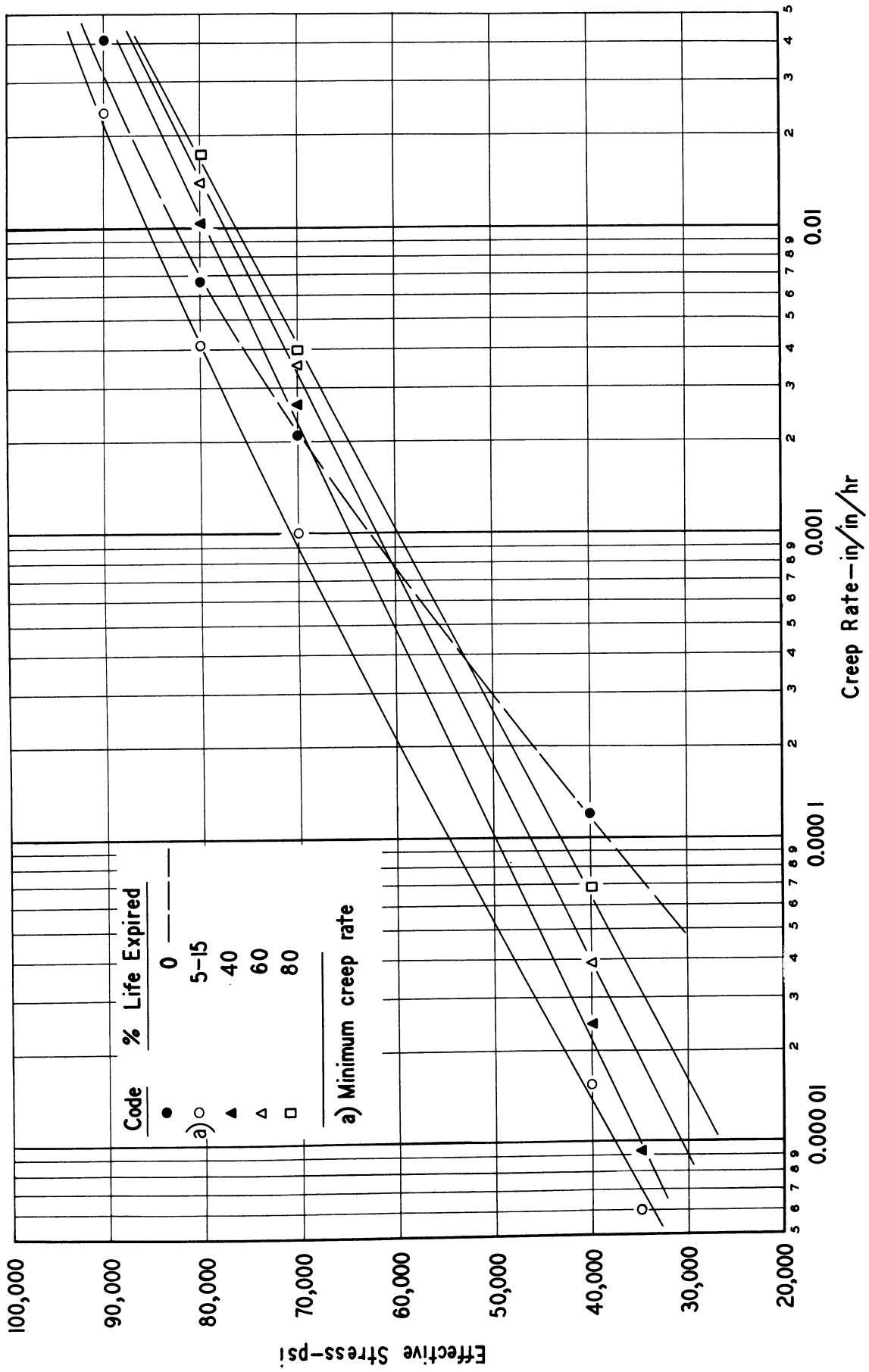

FIG.24 — STRESS VERSUS CREEP RATE AT 1350°F FOR WASPALOY (HEAT 44036) WITH CONVENTIONAL HEAT TREATMENT.

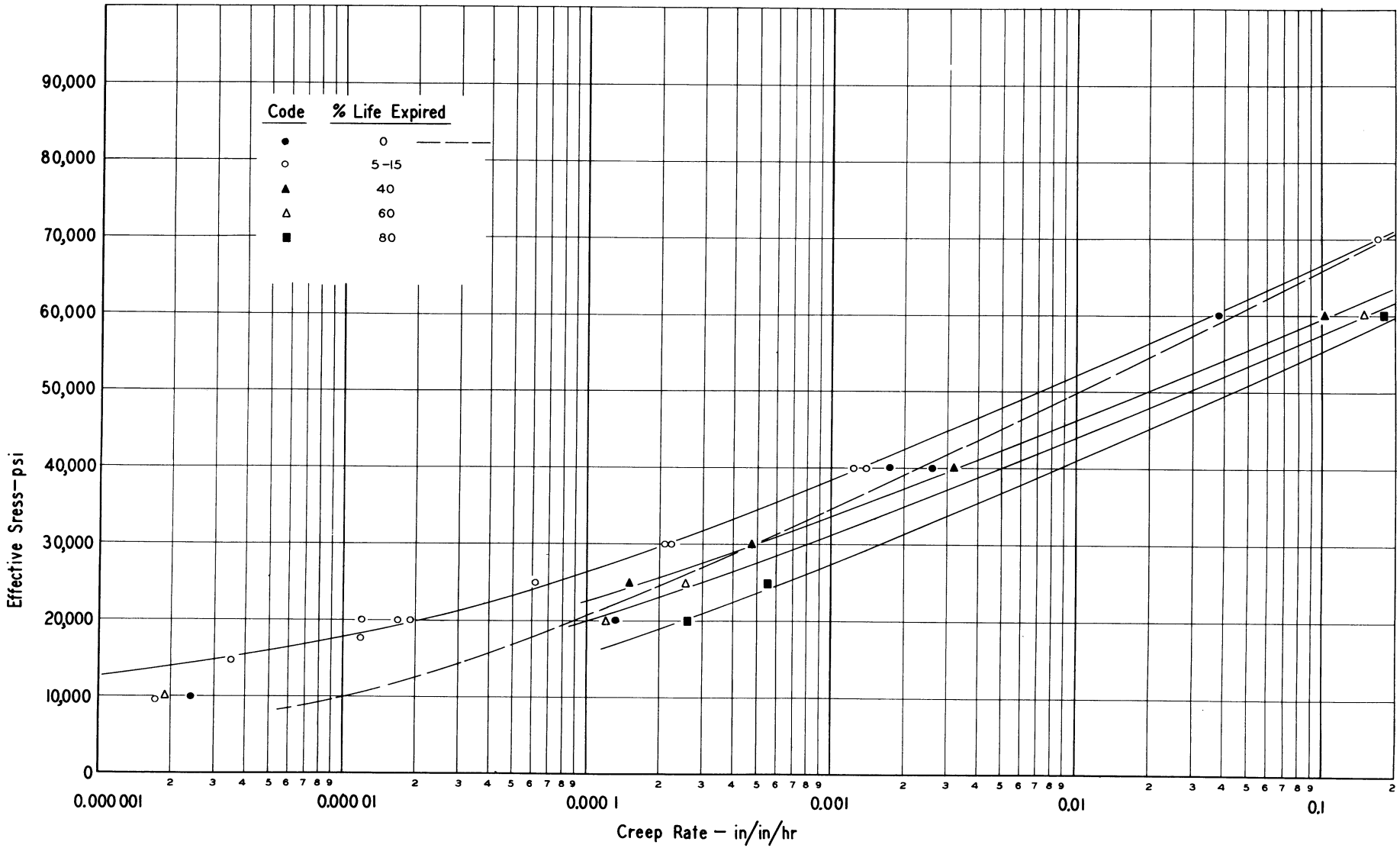

FIG.25-STRESS VERSUS CREEP RATE AT 1500°F FOR WASPALOY (HEAT 44036) WITH CONVENTIONAL HEAT TREATMENT.

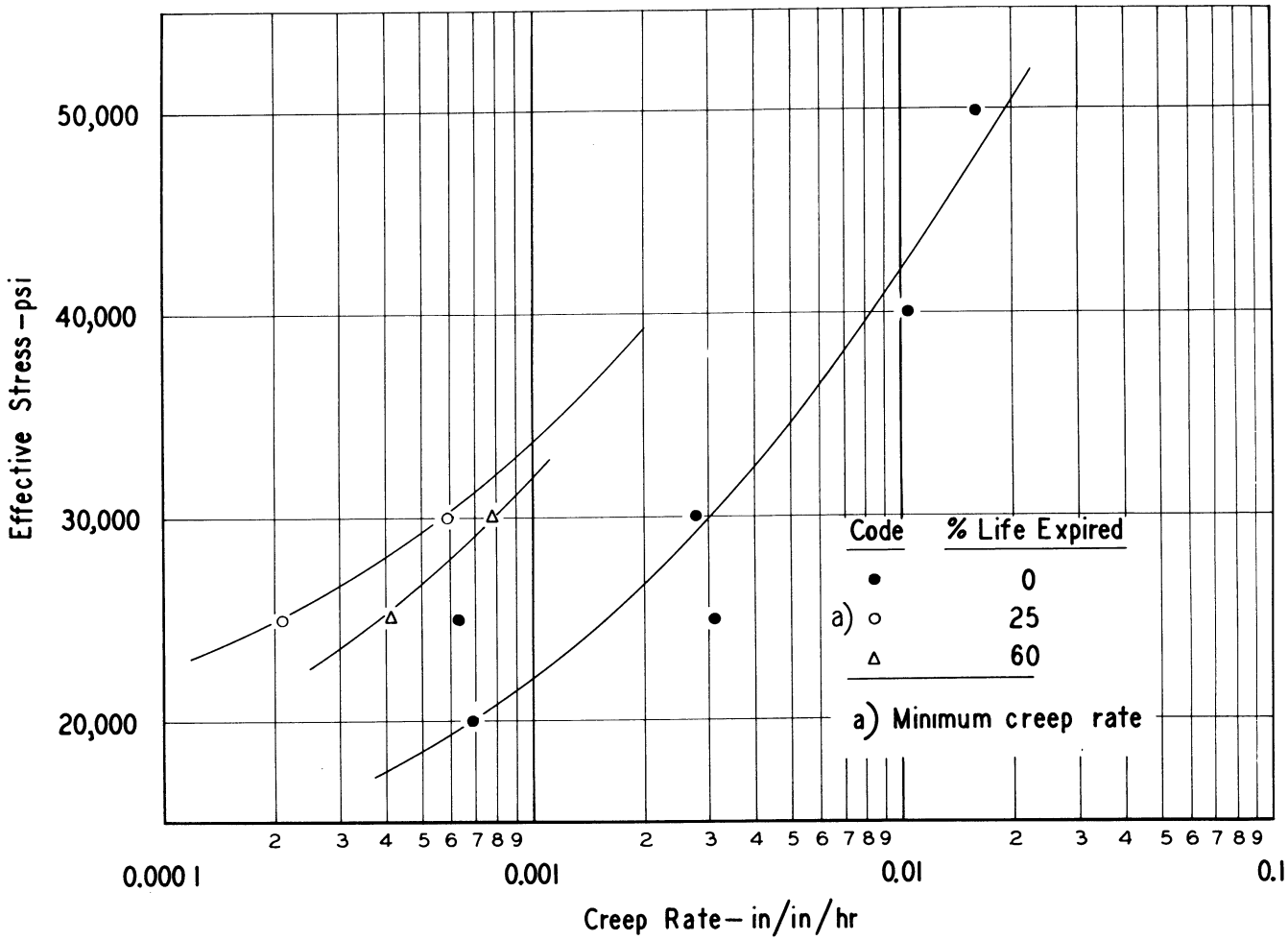

FIG.26 — STRESS VERSUS CREEP RATE AT 1500°F FOR WASPALOY ROLLED 15% AT ROOM TEMPERATURE BETWEEN CONVENTIONAL SOLUTION AND AGING TREATMENTS.

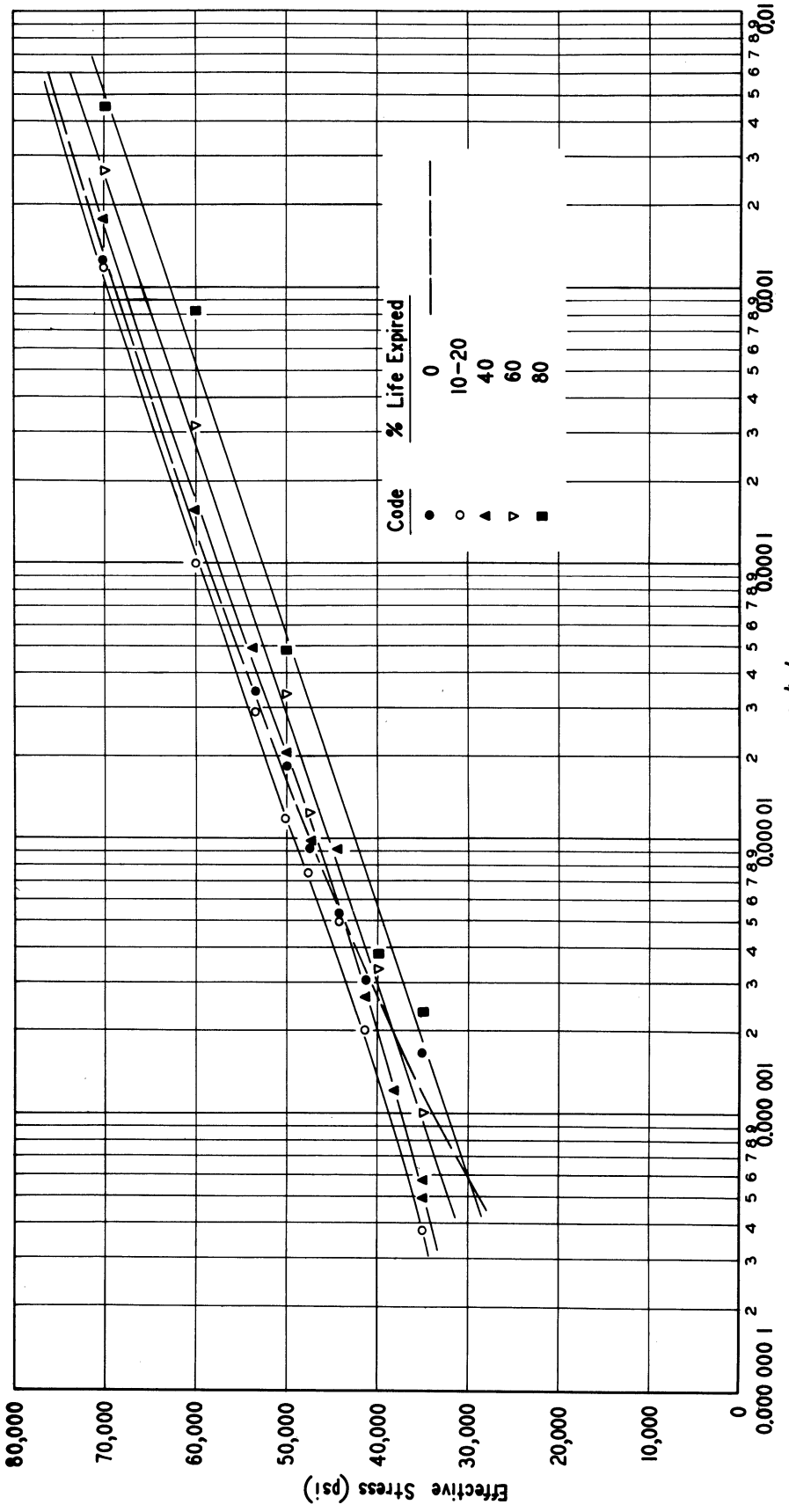

FIG. 27 — STRESS VERSUS CREEP RATE AT 1350°F FOR INCONEL X-550 WITH CONVENTIONAL HEAT TREATMENT.

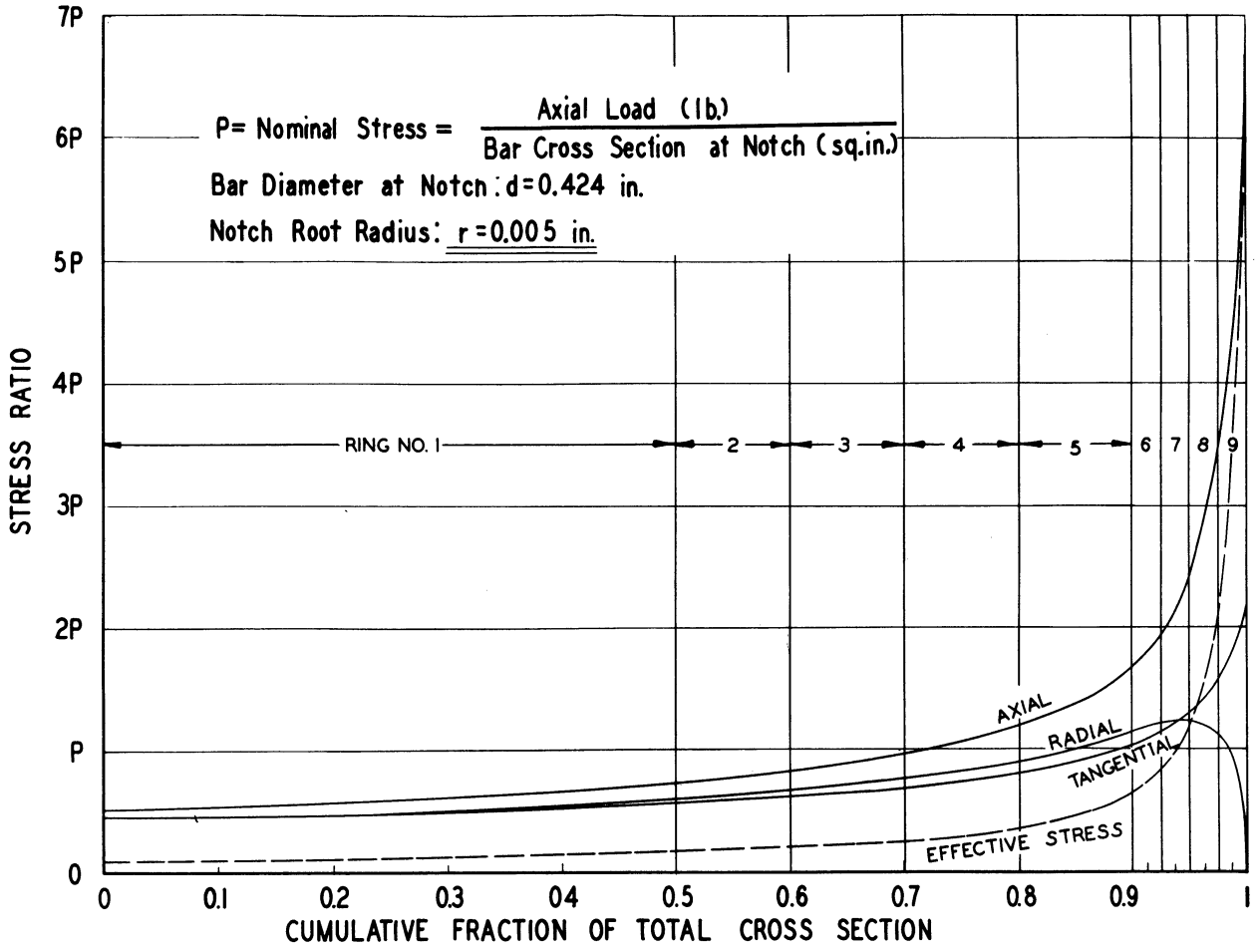

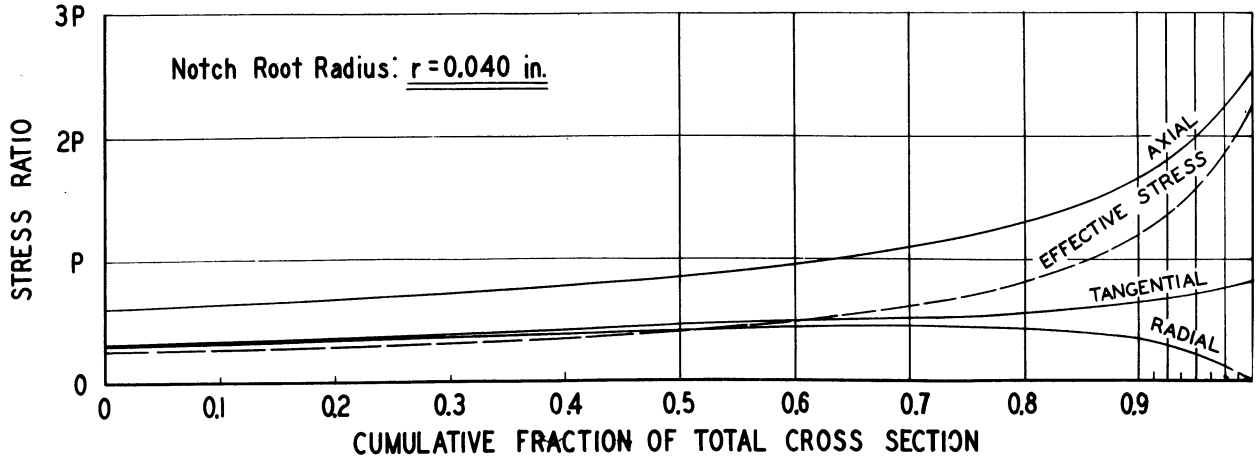

FIG.28– DISTRIBUTION OF ELASTIC STRESS COMPONENTS IN DEEP EXTERNAL CIRCUMFERENTIAL NOTCHES UNDER AXIAL TENSION.

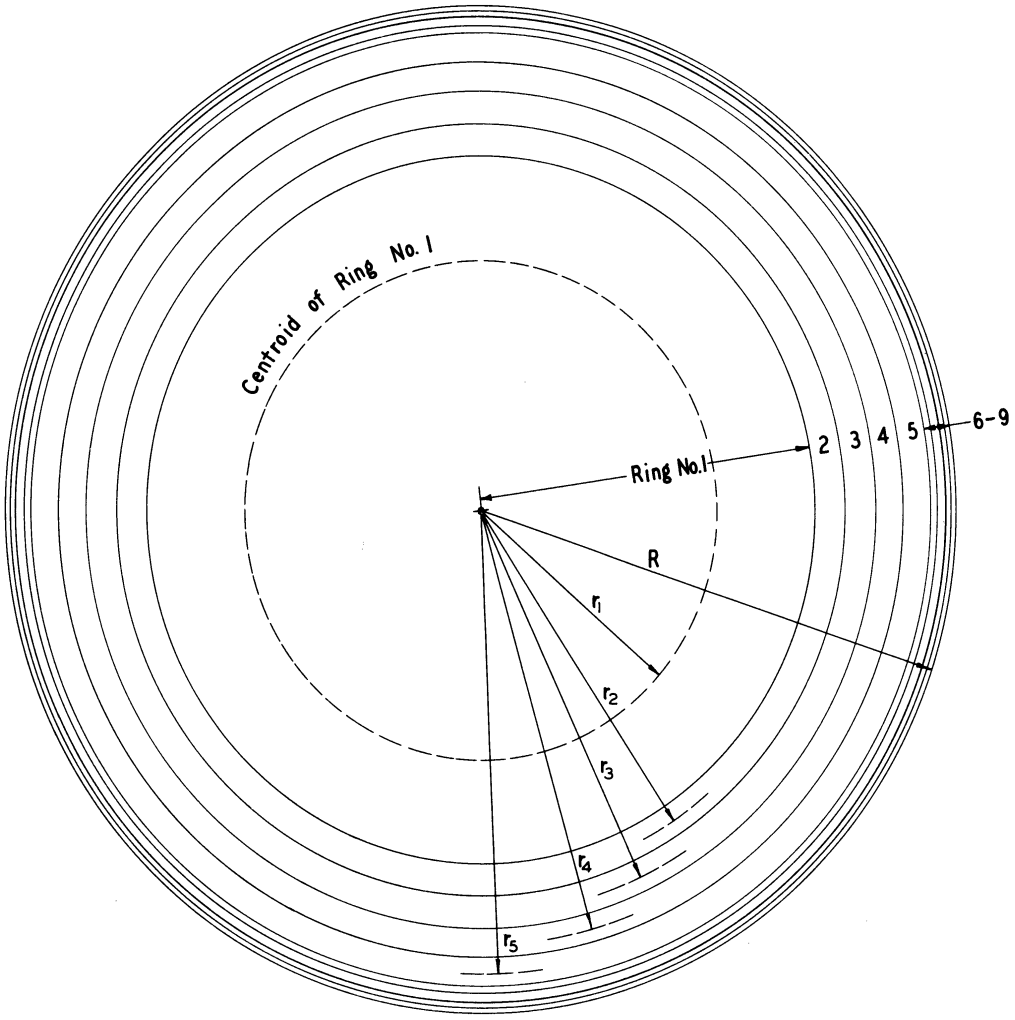

FIG.29 — SCHEME FOR DIVIDING PLANE OF NOTCH INTO RINGS FOR CALCULATION PURPOSES.

Ring No.	Centroid (r/R)	Area (Fraction of Total)
1	0.500	1/2
2	0.741	1/10
3	0.806	1/10
4	0.866	1/10
5	0.922	1/10
6	0.955	1/40
7	0.968	1/40
8	0.981	1/40
9	0.9936	1/40

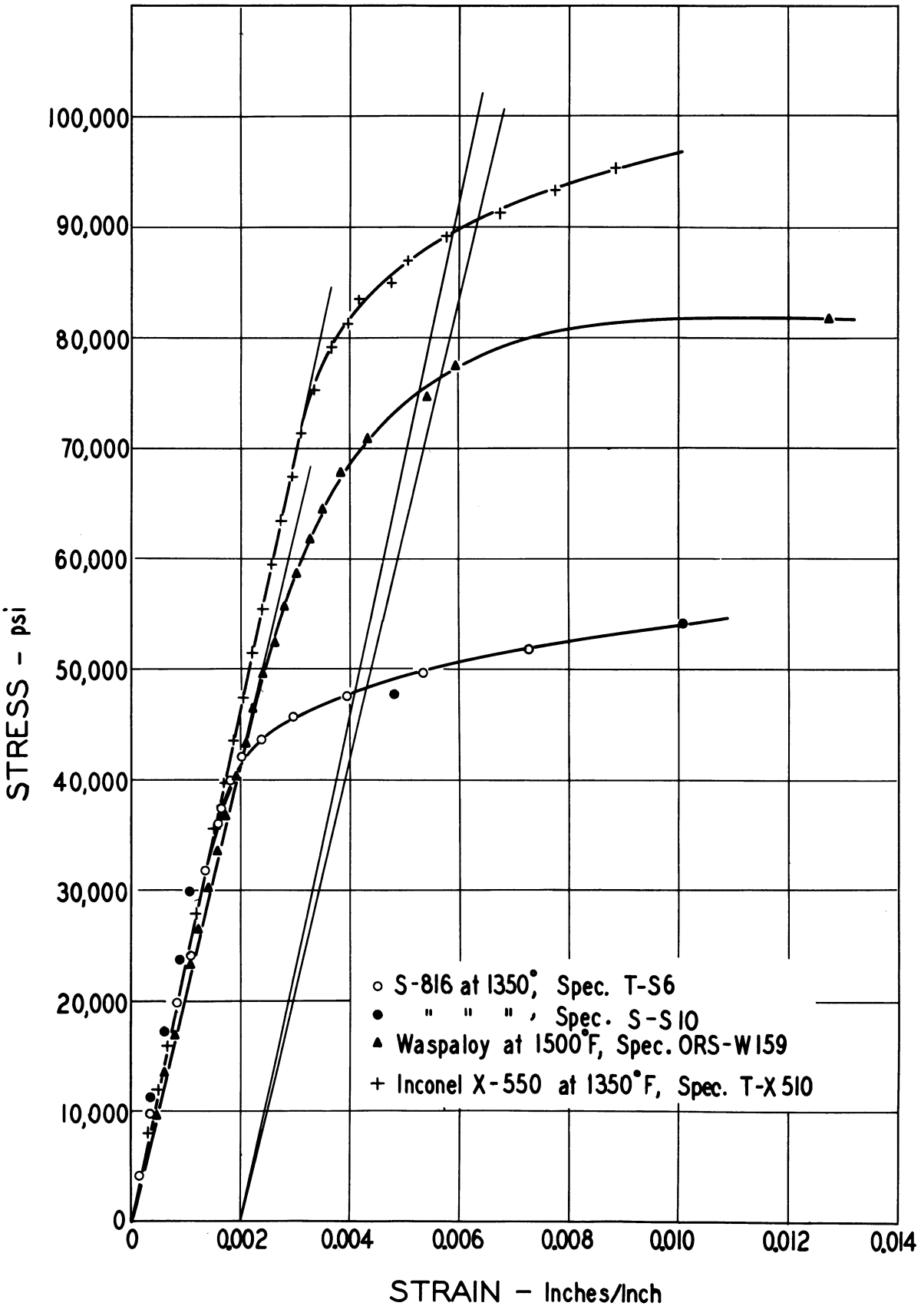

FIG. 30: SHORT-TIME TENSILE CHARACTERISTICS OF ALLOYS STUDIED.

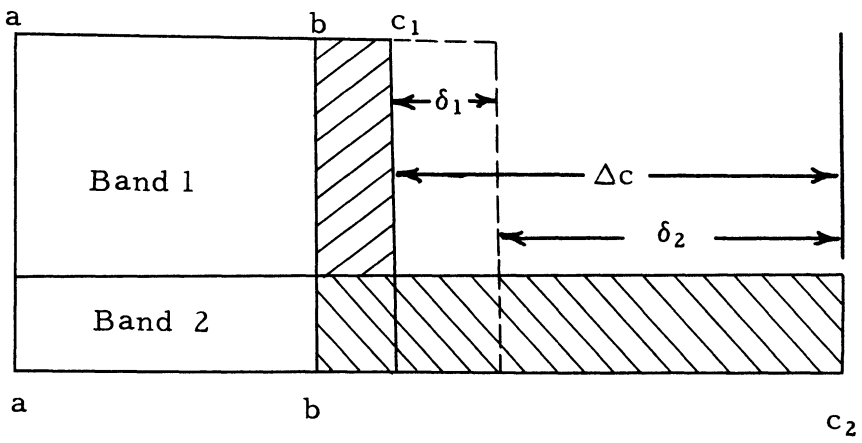

FIG. 31 - SCHEMATIC REPRESENTATION OF STRESS-STRAIN INTERACTIONS AT AN INTERFACE BETWEEN TWO BANDS WITH DIFFERENT CREEP RATES.

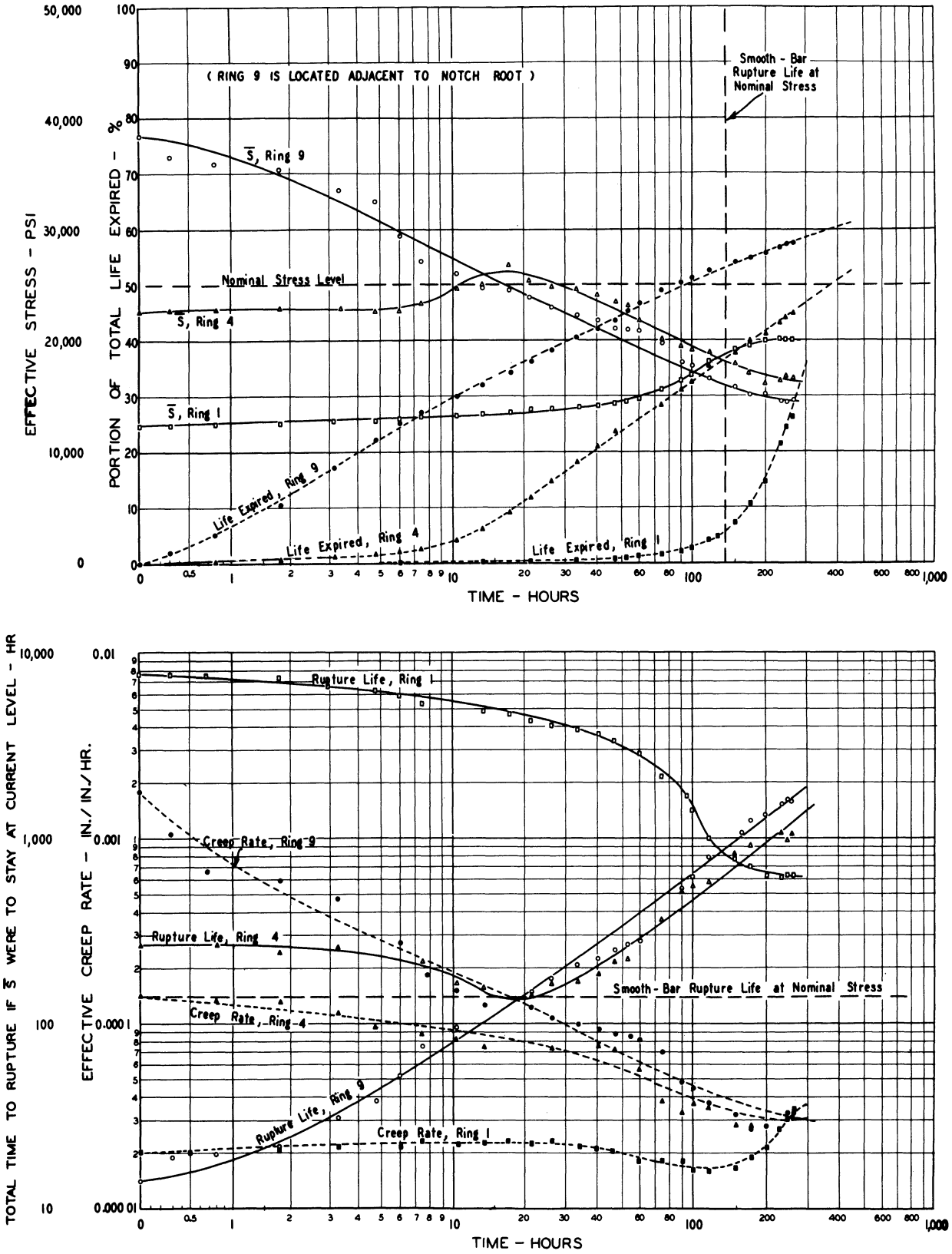

FIG. 32 – RESULTS OF STEPWISE CALCULATIONS BY PROPOSED CORRELATION BETWEEN NOTCH RUPTURE TESTS AND SMOOTH-BAR PROPERTIES (WASPALOY AT 1500°F, NOMINAL STRESS 25,000 PSI., NOTCH ROOT RADIUS 0.100 INCH.)

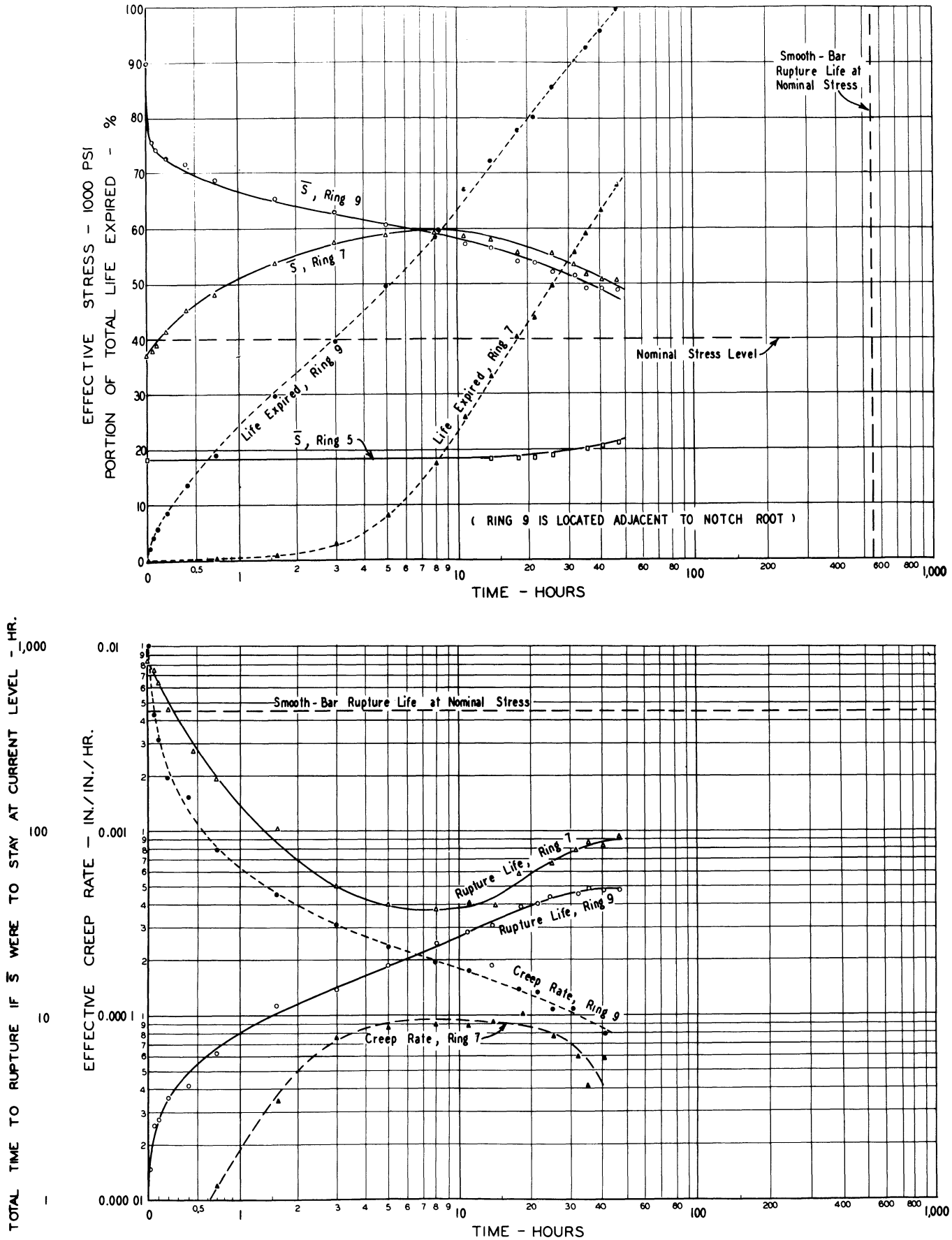

FIG. 33 — RESULTS OF STEPWISE CALCULATIONS BY PROPOSED CORRELATION BETWEEN NOTCH RUPTURE TESTS AND SMOOTH-BAR PROPERTIES. (INCONEL X-550 AT 1350°F, NOMINAL STRESS 40,000 PSI., NOTCH ROOT RADIUS 0.005 INCH.)

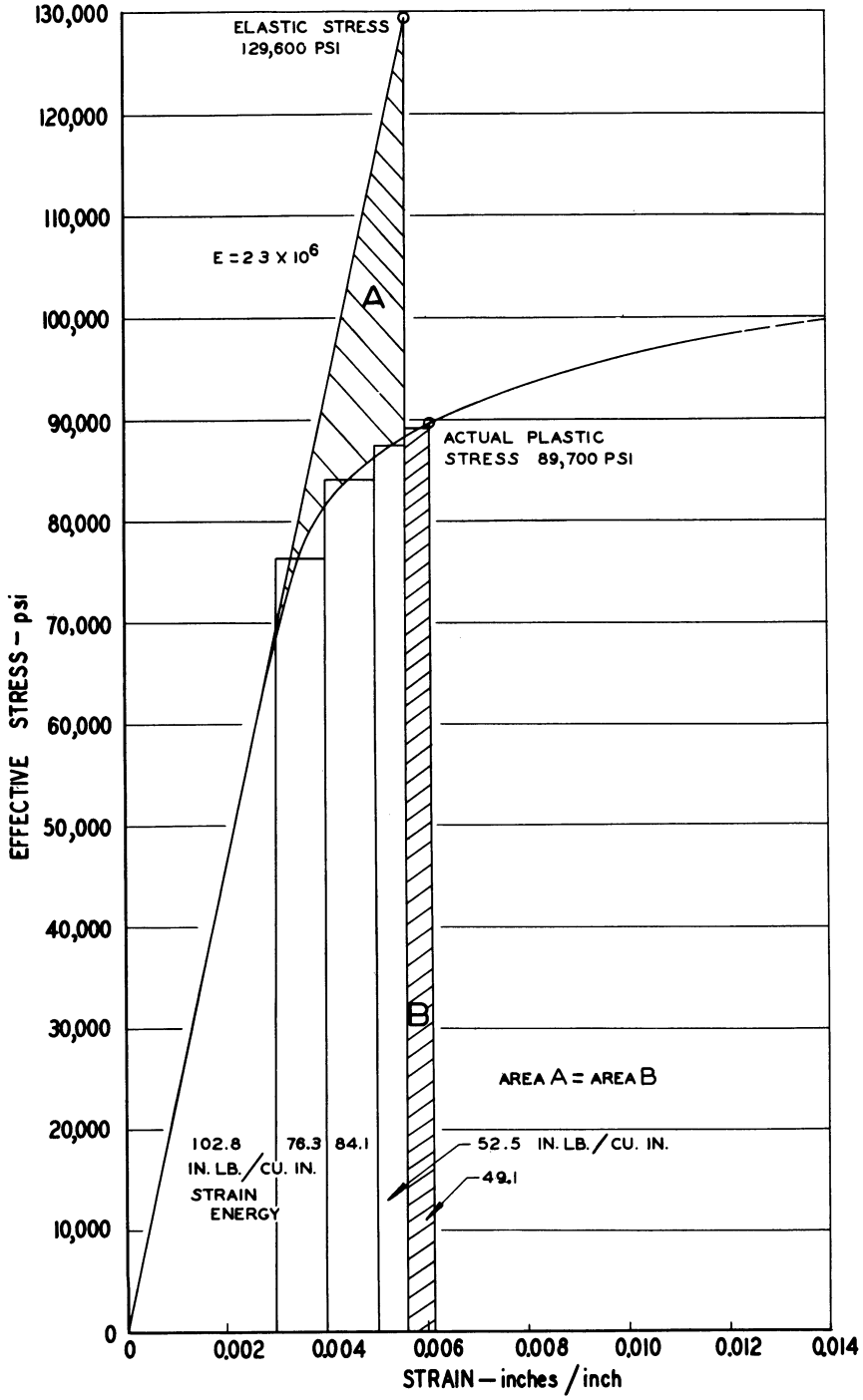

FIG.34 — STRESS-STRAIN CURVE FOR INCONEL X-550 AT 1350°F SHOWING ESTIMATION OF STRESS UNDER PLASTIC CONDITIONS WHEN THE ELASTIC STRESS CONCENTRATION FACTOR IS KNOWN.

NOMINAL STRESS: 40,000 PSI
NOTCH ROOT RADIUS: 0.005 IN.
DIAM. OF BAR AT NOTCH: 0.424 IN.
ELASTIC STRESS RATIO AT RADIUS IN QUESTION (RING NO. 9): 3.24